Lund University

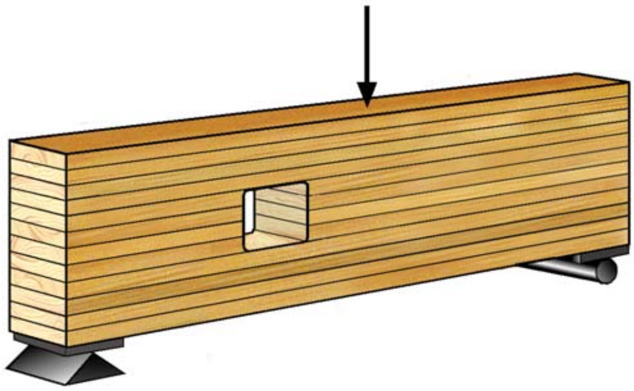

THE STRENGTH OF GLULAM BEAMS WITH HOLES
A Survey of Tests and Calculation Methods

HENRIK DANIELSSON

Structural Mechanics

Department of Construction Sciences
Structural Mechanics

ISRN LUTVDG/TVSM--07/3068--SE (1-91)
ISSN 0281-6679

THE STRENGTH OF GLULAM BEAMS WITH HOLES
A Survey of Tests and Calculation Methods

HENRIK DANIELSSON

Printed by KFS I Lund AB, Lund, Sweden, February 2009.

For information, address:
Division of Structural Mechanics, LTH, Lund University, Box 118, SE-221 00 Lund, Sweden.
Homepage: http://www.byggmek.lth.se

Abstract

A compilation of available test results relating to the strength of glulam beams with holes is presented. A total of 182 individual tests from 8 different sources are described concerning material, test setup and recorded crack loads and failure loads. A brief description of some available methods for strength analysis of timber is given and specific calculation approaches for the strength of glulam beams with holes are compiled. Design rules according to some European codes are reviewed and compared to experimental test results. Fundamentally different design approaches are found among the reviewed codes and the comparison reveals significant discrepancies between the predicted strengths according to the different codes.

Keywords: Glulam, beam, hole, strength, design, code.

Acknowledgements

This report was written during 2006 at the Division of Structural Mechanics at Lund University with financial support from Formas through grant 24.3/2003-0711.

I would like to express my gratitude to my supervisors Prof. Per Johan Gustafsson and Dr. Erik Serrano for their guidance and support during my first year of post graduate studies. I am also very thankful to Mr. Bo Zadig for helping med with graphics and printing and also to post graduate student Kirsi Salmela at the Swedish National Testing and Research Institute for translation of texts in Finnish. The good company and help received from the rest of the staff at the Division of Structural Mechanics are also gratefully acknowledged.

Lund, December 2006

Henrik Danielsson

Notations

Loads

P	Point load

Cross sectional forces

V_{c0}	Shear force at hole center at crack initiation
V_c	Shear force at hole center at crack through entire beam width
V_f	Shear force at hole center at failure
M_{c0}	Bending moment at hole center at crack initiation
M_c	Bending moment at hole center at crack through entire beam width
M_f	Bending moment at hole center at failure

Parameters describing beam and hole geometry

L	Length of span
L_{tot}	Total length of beam
H	Beam height
T	Beam width
l	Distance to center of hole from closest support
ϕ	Hole diameter of circular hole
a	Hole length of rectangular hole
b	Hole height of rectangular hole
c, d, e, f	Distances
g_P	Length of steel plate at point load
g_S	Length of steel plate at support
r	Radius of corners of rectangular holes
r_m	Radius of curvature for curved beams
n	Total number of tests in a beam series
i	Specific test number in a test series

Location of cracks

lb	Left bottom
lt	Left top
rb	Right bottom
rt	Right top
m	Failure due to bending (not at hole)

Material strength parameters

f_m	Bending strength
$f_{t,0}$	Tensile strength parallel to grain
$f_{t,90}$	Tensile strength perpendicular to grain
$f_{c,0}$	Compressive strength parallel to grain
$f_{c,90}$	Compressive strength perpendicular to grain
f_v	Shear strength
f_R	Rolling shear strength
$f_{*,*,k}$	Characteristic strength
$f_{*,*,d}$	Design strength

Material stiffness parameters

$E_\parallel$	Young's modulus parallel to grain
$E_\perp$	Young's modulus perpendicular to grain
G	Shear modulus
G_R	Rolling shear modulus
ν	Poisson's ratio

Fracture mechanics parameters

G_f	Fracture energy
K_i	Stress intensity factor
K_{ic}	Critical stress intensity factor (Fracture toughness)
G_i	Energy release rate (Crack driving force)
G_{ic}	Critical energy release rate (Crack resistance)
	i=I, II, III depending on mode of loading
J	J-integral
J_c	Critical value of J-integral
x_m	Integration length for mean stress method
a_0	Length of fictitious crack for initial crack method
k	Mixed mode ratio

Contents

Chapter 1

Introduction

1.1 Background

The mechanical properties of wood are very different for different type and orientation of stresses. Wood is very weak when exposed to tensile stress perpendicular to grain. Hence, special attention should be given when designing a timber structure in order to avoid these stresses but this is however not always possible. It is for example many times necessary, or at least desirable, to make holes through glulam beams. Introducing a hole in a glulam beam significantly changes the distribution of stresses in the vicinity of the hole. Tensile stresses perpendicular to grain appear and the capacity of the beam can accordingly be decreased. The perpendicular to grain tensile type of fracture is moreover commonly very brittle which means that safe strength design is of outmost importance. Two examples of constructions with glulam beams with holes are shown in Figure 1.1.

1.2 Aim and scope

The aim of this report is first and foremost to compile as many as possible of the performed full scale tests of the capacity of glulam beams with a hole. The compilation deals almost exclusively with unreinforced holes but extensive testing has also been carried out on glulam beams with holes reinforced in different ways. An example of the test setup for a full scale test is shown in Figure 1.2.

A secondary aim is to give an overview of available methods for tensile fracture analysis of wooden structural elements and in particular a brief summary of approaches presently and previously used to estimate the load bearing capacity for glulam beams with holes. A review of design recommendations concerning glulam beams with holes according to different European codes is also presented as well as a comparison of these recommendations with test results.

Figure 1.1: *Examples of constructions with glulam beams with holes. Top: Restaurant Ideon, Lund, Sweden. Bottom: Indoor swimming pool, Västerås, Sweden (with permission from Martinsons Trä AB).*

Figure 1.2: *Full scale test glulam beam with holes, MPA Stuttgart [32]*

1.3 Disposition

This report is organized as follows. A short introduction to the topic is given in Chapter 1. Then, in Chapter 2, test results relating to the strength of glulam beams with one or more holes found in literature are presented and summarized. Chapters 3, 4 and 5 deals with methods for of calculation; methods of tensile fracture of wood analysis in general (Chapter 3), methods used for calculating the strength of glulam beams with holes (Chapter 4) and design rules according to some European codes (Chapter 5). Some concluding remarks are presented in Chapter 6.

Chapter 2

Experimental tests

2.1 General remarks

A compilation of tests on glulam beams with circular or rectangular holes is presented with a total of 182 tests from 8 different sources. The tests from each source are described in separate sections concerning material, test setup and results. All test results are also summarized in the end of this chapter. The materials are described in terms of strength class, moisture content and sometimes additional information depending on what is specified in the original source.

The test setups used can all be narrowed down to five setups according to Figures 2.1, 2.2, 2.3, 2.4 and 2.5. In order to present all tests in a convenient and consistent way, two types of tables are used; *Beam geometry and test setup*-tables and *Hole design and test result*-tables.

A *Beam geometry and test setup*-table of principle is shown in Table 2.1. The tests are divided into *Beam series* which is a series of beams with identical beam geometry; L, L_{tot}, H, T, c, d, e, f, g_P and g_S. They are given names corresponding to the first three letters in the author's name or one of the authors' names and sometimes followed by letters a - f when there are several series from the same author/authors. The number n in the table is the number of tests performed in the *Beam series* (i.e. on the same beam geometry). Several different hole designs are often tested within the same beam series. The design of the holes and results of the tests are presented in the *Hole design and test result*-tables which looks like Table 2.2. The first column of these tables holds the *Test series notation*, which is the name of the *Beam series* followed by a number where all tests with the same number are identical with respect to test setup, beam geometry and also hole design. The notation from the original source (if there is one) is given in the second column. The third column holds parameters describing the design of the tested hole according to Figure 2.6. The distance from closest support to center of hole l and the bending moment to shear force ratio $M/(VH)$ at hole center are presented in the fourth and fifth columns respectively. The specific test number i is given in the sixth column. Columns 7-9 hold values of the shear force or the bending moment and the last column shows the location of cracks (LoC) which are defined in Figure 2.6.

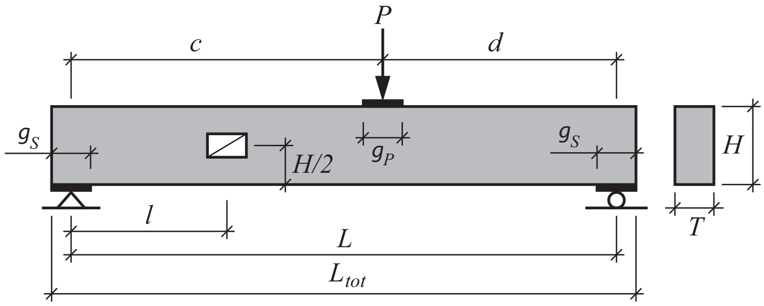

Figure 2.1: *Test setup 1.*

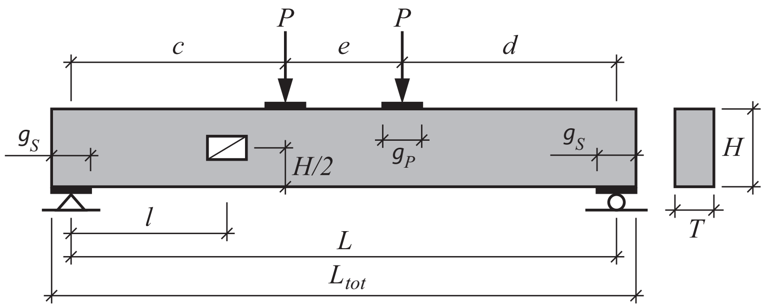

Figure 2.2: *Test setup 2.*

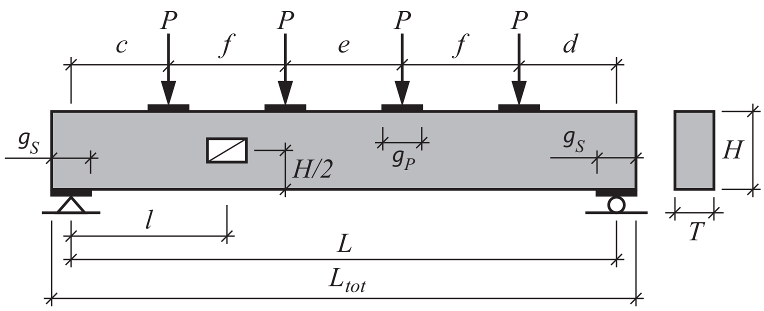

Figure 2.3: *Test setup 3.*

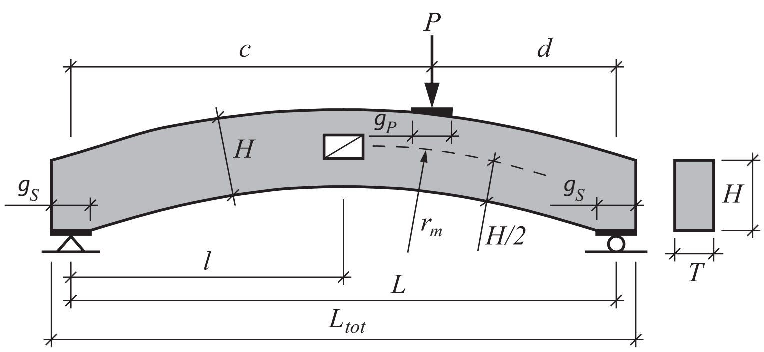

Figure 2.4: *Test setup 4.*

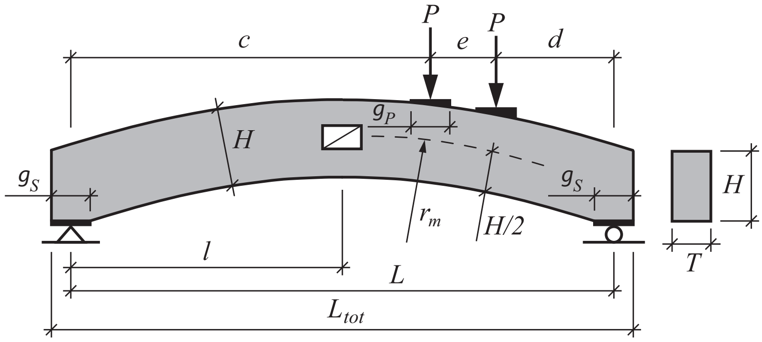

Figure 2.5: *Test setup 5.*

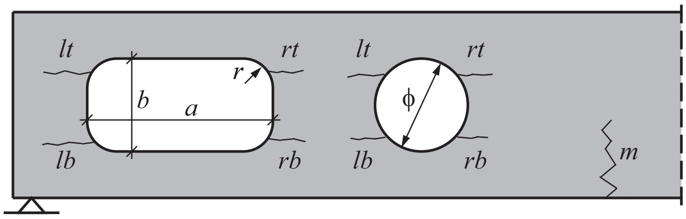

Figure 2.6: *Notations for hole dimensions and location of cracks.*

Table 2.1: *Beam geometry and test setup, Author's name or Authors' names, Year.*

Beam series	Test setup	n	L_{tot} [mm]	L [mm]	$H \times T$ [mm^2]	c [mm]	d [mm]	e [mm]	f [mm]	g_P [mm]	g_S [mm]
XXX(x)	1, 2, 3 4 or 5		Geometry parameters according to Figure 2.1, 2.2 or 2.3								

Table 2.2: *Hole design and test results, Author's name or Authors' names, Year.*

For holes placed in shear force dominated regions

Test series notation	Original test notation	Hole design ϕ or $a \times b,\ r$ [mm]	l [mm]	$\frac{M}{VH}$ [-]	i	V_{c0} [kN]	V_c [kN]	V_f [kN]	LoC
XXX(x)-N					1 2 ⋮ mean std				

For holes placed in pure moment regions

Test series notation	Original test notation	Hole design ϕ or $a \times b,\ r$ [mm]	l [mm]	$\frac{M}{VH}$ [-]	i	M_{c0} [kNm]	M_c [kNm]	M_f [kNm]	LoC
XXX(x)-N				∞	1 2 ⋮ mean std				

The extent of presented test data vary significantly between the various sources. Some of the authors present only the ultimate loads or the loads when cracks start to appear, while others present several levels of the load during the test procedure. The authors of the sources used in the compilation have further not used exactly the same definitions of the different load levels and sometimes the definitions are rather unclear. Hence, some simplifications are almost inevitable in order to compile all test in a convenient way. In this report, three different load levels denoted V_{c0}, V_c and V_f are defined according to Figure 2.7. The shear force at crack initiation V_{c0} is defined as the shear force at hole center when a crack opens up but does not yet spread across the entire beam width. V_c is defined as the shear force at hole center when the crack has propagated over the entire beam width and V_f is defined as the shear force at failure. Failure can be due to crack propagation to the very end of the beam or global bending failure. For hole placed in pure moment regions, the corresponding definitions of bending moments M_{c0}, M_c and M_f are used. When the definitions used in the original source are unclear or do not quite agree with the definitions stated above, the test results are compiled in what is thought to be the best possible way. The values of the cross sectional forces are presented as reported in the original sources. No corrections due to influence of the dead-weight of the beams are added in this compilation.

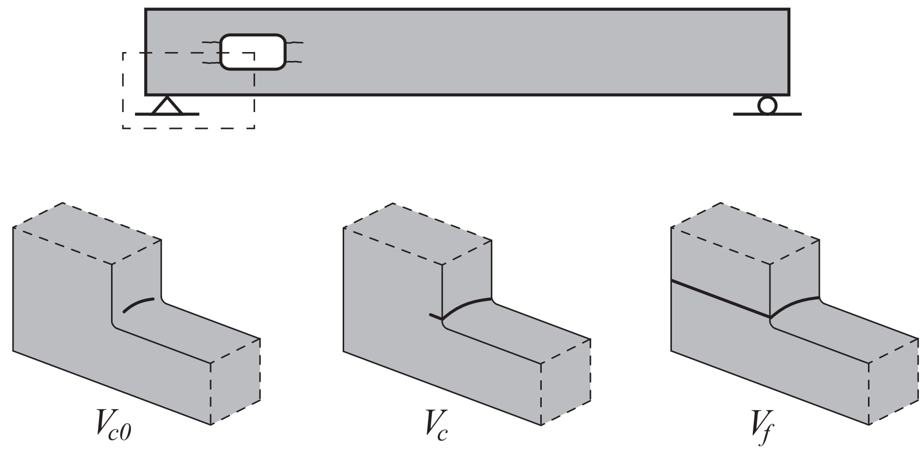

Figure 2.7: *Illustration of crack patterns for crack location lb at load levels* V_{c0}, V_c and V_f. *The same crack patterns are valid for crack locations lt, rb and rt.*

Some tests are very closely described concerning beam geometry, material and test setup while others are described in a more brief manner. In the case when some parameters are not specified in the original source, a question mark (?) is used in the tables. Furthermore, the tests have been performed at different locations by different personnel which means that there might be a significant variation in the test procedures. These are some important remarks to keep in mind when reading this report. Material strength- and stiffness properties of glulam strength classes as defined in various codes are presented in Table 2.3. The glulam strength classes included in the table presented are those used in the tests.

Table 2.3: *Material properties of used glulam strength classes.*

	BKR [35] L40	**SS-EN 1194** [40] GL32h	**DIN 1052** [33] GL32h	**SIA 164**[5] [37] Klasse B
Characteristic strengths [MPa]				
f_m	33[1]	32[1]	32[1]	12
$f_{t,0}$	23[1]	22.5[1]	22.5	10
$f_{t,90}$	0.5	0.5	0.5	0.15
$f_{c,0}$	36	29	29	10
$f_{c,90}$	8	3.3	3.3	?
f_v	4[2]	3.8	3.5	1.2
f_R	2		1.0	1
Stiffness properties [MPa]				
$E_{\parallel}$	13000	13700[3]	13700[4]	10000
$E_{\perp}$	450	460[3]	460[4]	300
G	850	850[3]	850[4]	500
G_R			85	

[1] = For beams with height $\geq$ 600 mm.
[2] = For beams with rectangular cross section
[3] = Mean value.
[4] = Mean value, characteristic value = $5/6 \cdot$ mean value
[5] = Allowable stress according to SIA 164.

2.2 Bengtsson and Dahl, 1971

Bengtsson and Dahl performed tests on glulam beams with holes within their master's dissertation *Inverkan av hål nära upplag på hållfastheten hos limträbalkar* (Influence of holes near support on the strength of glulam beams) [4] from 1971. Reinforced and unreinforced holes of different sizes and shapes were tested. The reinforcement consisted of 10 mm thick plywood boards which were glue-nailed to both sides of the beams.

Material

All beams were delivered by *AB Fribärande Konstruktioner Töreboda*, of strength class L40 and made of spruce. The beams where kept at constant climate for six weeks prior to testing and the average moisture content at testing was 9-10 %.

Test Setup

A total of six beams with two symmetrically placed holes each were tested. The beams where tested in a three-point-bending test according to Figure 2.1. The dimensions of the used glulam beams are presented in Table 2.4. Both circular and rectangular holes were investigated. For the rectangular holes, the corners were not rounded but were instead sharp. The beams were all stabilized in the weak direction at the two supports and also at the middle where the point load acted. Strains were measured at one of the two holes of each beam. If failure occurred at the hole where strains were not measured, the beam was mended at this hole and then loaded again. This procedure resulted in two values of the failure load for some of the beams.

Table 2.4: *Beam geometry and test setup, Bengtsson and Dahl, 1971.*

Beam series	Test setup	n	L_{tot} [mm]	L [mm]	$H \times T$ [mm^2]	c [mm]	d [mm]	e [mm]	f [mm]	g_P [mm]	g_S [mm]
BEN	1	9	5300	5000	500×90	2500	2500	-	-	?	?

Results

The hole designs and test results are shown in Table 2.5. Bengtsson and Dahl recorded and presented the "failure loads" for all beams but there is no explicit definition of this load. It is also stated that cracks appeared at load levels of 70-90 % of the "failure loads" in most of the tests. The recorded loads are thus assumed to correspond to the definition of V_f in this report.

Table 2.5: *Hole design and test results, Bengtsson and Dahl, 1971.*

Test series notation	Original test notation	Hole design ϕ or $a \times b,\ r$ [mm]	l [mm]	$\frac{M}{VH}$ [-]	i	V_{c0} [kN]	V_c [kN]	V_f [kN]	LoC
BEN-1	A1	$\phi 250$	600	1.20	1			37.5	lb,rt
					2			39.2	lb,rt
					mean			38.4	
					std			1.2	
BEN-2	B1	$300 \times 150,\ 0$	600	1.20	1			38.8	lb,rt
					2			39.2	lb,rt
					mean			39.0	
					std			0.3	
BEN-3	C	$\phi 150$	600	1.20	1			52.5	m
BEN-4	D	$200 \times 100,\ 0$	600	1.20	1			48.8	lb,rt
					2			50.3	lb,rt
					mean			49.6	
					std			1.1	
BEN-5[1]	A2	$\phi 250$	600	1.20	1			55.0	m
BEN-6[1]	B2	$300 \times 150,\ 0$	600	1.20	1			78.5	lb,rt

[1] = Reinforced hole

2.3 Kolb and Frech, 1977

Tests on glulam beams with holes are presented in *Untersuchungen an durchbrochenen Bindern aus Brettschichtholz* (Analyses of glulam beams with holes) [20] by Kolb and Frech from 1977. Both reinforced holes and unreinforced holes were tested but the tests on reinforced holes are not included in this compilation.

Material

The lamellae thickness was 29 mm and the moisture content at the time of testing was 10 %. The properties of the glulam is not further specified.

Test setup

A total of six different configurations concerning hole geometry and placement for unreinforced holes were tested. Each configuration was applied to two beams resulting in a total of 12 tests as can be seen in Table 2.6. The tests were all performed as four-point-bending test according to Figure 2.2 with the hole placed in a shear force dominated region or placed in a region with pure bending moment. The holes seem to have had rounded corners but the radius is not to be found in the paper.

Table 2.6: *Beam geometry and test setup, Kolb and Frech, 1977.*

Beam series	Test setup	n	L_{tot} [mm]	L [mm]	$H \times T$ [mm^2]	c [mm]	d [mm]	e [mm]	f [mm]	g_P [mm]	g_S [mm]
FRE	2	12	8400	8000	550×80	2000	2000	4000	-	?	?

Results

The hole designs and the results are presented in Table 2.7. The recorded loads are maximum loads. For the beams with holes placed in shear force dominated region, the maximum load corresponds to crack growth from hole to end of beam. For the beams with a hole placed in pure moment region the capacities were limited by bending failure at midspan.

Table 2.7: *Hole design and test results, Kolb and Frech, 1977.*

Test series notation	Original test notation	Hole design ϕ or $a \times b,\ r$ [mm]	l [mm]	$\frac{M}{VH}$ [-]	i	V_{c0} [kN]	V_c [kN]	V_f [kN]	LoC
FRE-1	II-D	$250 \times 250,\ ?$	500	0.91	1			31.2	lb,rt
					2			34.2	lb,rt
					mean			32.7	
					std			2.1	
FRE-2	II-G	$250 \times 150,\ ?$	500	0.91	1			42.0	lb,rt
					2			46.0	lb,rt
					mean			44.0	
					std			2.8	
FRE-3	II-E	$250 \times 250,\ ?$	1000	1.82	1			33.0	lb,rt
					2			34.6	lb,rt
					mean			33.8	
					std			1.1	
FRE-4	II-H	$250 \times 150,\ ?$	1000	1.82	1			38.2	lb,rt
					2			32.6	lb,rt
					mean			35.4	
					std			4.0	
Test series notation	Original test notation	Hole design ϕ or $a \times b,\ r$ [mm]	l [mm]	$\frac{M}{VH}$ [-]	i	M_{c0} [kNm]	M_c [kNm]	M_f [kNm]	LoC
FRE-5	III-C	$\phi 300$	4000	∞	1			140.0	m
					2			140.0	m
					mean			140.0	
					std			0.0	
FRE-6	III-D	$300 \times 300,\ ?$	4000	∞	1			133.6	m
					2			140.0	m
					mean			136.8	
					std			4.5	

2.4 Penttala, 1980

Tests on glulam beams with holes have been carried out at Helsinki University of Technology. The results are presented by Penttala in the report *Reiällinen liimapuupalkki* (Glulam beams with holes) [21] from 1980.

Material

The material used for the glulam beams are of quality L40D with 33 mm thick lamellae. The beams were kept in indoor climate three weeks prior to the tests resulting in a moisture content of 8.2 % (std 0.3 %). The mean density for the beams was 457.8 kg/m^3 (std 36.2 kg/m^3).

Test setup

The test series consist of tests on two different beam geometries concerning cross section and length and also on circular as well as on rectangular holes. A total of ten tests were carried out. All tests were performed as three-point-bending test according to Figure 2.1 with the hole located in a region subjected to both shear force and bending moment. The geometries of the beams are presented in Table 2.8. The corners of the rectangular holes seem to have been rounded but the radius is not specified in the report.

Table 2.8: *Beam geometry and test setup, Penttala, 1980.*

Beam series	Test setup	n	L_{tot} [mm]	L [mm]	$H \times T$ [mm^2]	c [mm]	d [mm]	e [mm]	f [mm]	g_P [mm]	g_S [mm]
PENa	1	6	4300	4000	500×90	2000	2000	-	-	?	?
PENb	1	4	5400	5000	800×115	2500	2500	-	-	?	?

Results

The hole designs and test results are presented in Table 2.9. Two load levels were defined; load at first visible crack and load at failure which here corresponds to the definitions of V_{c0} and V_f.

Table 2.9: *Hole design and test results, Penttala, 1980.*

Test series notation	Original test notation	Hole design ϕ or $a \times b,\ r$ [mm]	l [mm]	$\frac{M}{VH}$ [-]	i	V_{c0} [kN]	V_c [kN]	V_f [kN]	LoC
PENa-1	P-1	ϕ255	600	1.20	1			33.8	lb,rt
PENa-2	P-2	ϕ250	1050	2.10	1			31.6	lb,rt
PENa-3	P-3	ϕ150	600	1.20	1			51.3	lb,rt
PENa-4	P-6	200 × 200, ?	800	1.60	1			33.8	lb,rt
PENa-5	P-7	400 × 200, ?	800	1.60	1	25.0		31.3	lb,rt
PENa-6	P-8	600 × 200, ?	600	1.60	1	20.8		30.0	lb,rt
PENb-1	P-4	ϕ400	820	1.03	1	57.1		65.9[1]	lb,rt
PENb-2	P-5	ϕ300	1600	2.00	1			89.5	lb,rt
PENb-3	P-9	400 × 200, ?	1000	1.25	1			69.1	lb,rt
PENb-4	P-10	200 × 200, ?	1000	1.25	1	52.5		84.4	lb,rt

[1] = Failure by crack propagation due to poor glue line bonding.

2.5 Johannesson, 1983

Johannesson has performed several series of tests on glulam beams with holes which are presented in the doctoral thesis *Design problems for glulam beams with holes* [14] from 1983. A total of 45 unreinforced glulam beams with varying cross section, hole types and hole placement were tested. Out of these 45 tests, one test in long term loading is excluded but the remaining 44 test are included in this compilation. Five papers are appended to the doctoral thesis, three of which concerns tests performed by Johannesson, one concerning tests presented by other authors and one concerning calculation methods for glulam beams with holes.

2.5.1 Paper I

Paper I is titled *Holes in Plywood Beams and Glued Laminated Timber Beams* [15] and presents 13 tests on glulam beams with circular and rectangular holes.

Material

All beams were of strength class L40, made of Swedish spruce (Lat. *Picea Abies*) and glued with a phenol-resorcinol glue. Two different lamellae thicknesses were used, 33 1/3 mm and 45 mm. The placements of the holes were made in order to avoid big knots where cracks were expected to appear. The beams were prior to testing kept in an environment of 20-22 °C and RH 60-70 % which resulted in a moisture content of 11-15 % in the beams at the time of testing.

Test Setup

The tests were performed on six different beams with a total of 13 holes. For five out of the six beams, two holes were tested for each beam. These beams were loaded with a single point load at midspan and the holes were all placed in the shear force dominated region of the beam. The beams were made with a total length greater than the span which made it possible to test two holes for each beam but still having only one hole in the stressed part of the beam for each test. In the sixth beam, a third hole was also made. This hole was placed at midspan and the beam was subjected to one point load on each side of the hole which means the hole is placed in an almost pure moment region of the beam. This test arrangement thus results in 13 separate tests, according to Table 2.10. The test setups and notations are shown in Figures 2.1 and 2.2. The corners of the rectangular holes were rounded with a radius of 25 mm and all hole surfaces were smoothed with sandpaper.

Table 2.10: *Beam geometry and test setup, Johannesson I, 1983.*

Beam series	Test setup	n	L_{tot} [mm]	L [mm]	$H \times T$ [mm^2]	c [mm]	d [mm]	e [mm]	f [mm]	g_P [mm]	g_S [mm]
JOHa	1	12	-	5000	500×90	2500	2500	-	-	?	?
JOHb	2	1	-	5000	500×90	2000	2000	1000	-	?	?

Results

The hole designs and the results of these beam series are presented in Table 2.11. The definitions used by Johannesson in Paper I do not correspond exactly to the definitions used in this report in the sense that there is no distinction between V_{c0} and V_c. The loads presented in the original source as ”load at first visible crack” are here viewed as V_c. The loads here presented as failure loads V_f are in the original source defined as the load when it was impossible to further increase the load due to beam deflection. Location of cracks are not specified for each individual test but are given as principal locations.

Table 2.11: *Hole design and test results, Johannesson I, 1983.*

Test series notation	Original test notation	Hole design ϕ or $a \times b,\ r$ [mm]	l [mm]	$\frac{M}{VH}$ [-]	i	V_{c0} [kN]	V_c [kN]	V_f [kN]	LoC
JOHa-1	L1	$\phi 250$	650	1.30	1		25.7	39.5	lb,rt
					2		33.4	33.4	lb,rt
					mean		29.6	36.5	
					std		5.4	4.3	
JOHa-2	L2	$250 \times 250,\ 25$	650	1.30	1		27.1	30.5	lb,rt
					2		26.4	26.5	lb,rt
					mean		26.8	28.5	
					std		0.5	2.8	
JOHa-3	L3	$\phi 250$	1400	2.80	1		35.0	35.0	lb,rt
					2		31.3	39.9	lb,rt
					mean		33.2	37.5	
					std		2.6	3.5	
JOHa-4	L4	$250 \times 250,\ 25$	1400	2.80	1		23.8	26.0	lb,rt
					2		20.5	25.2	lb,rt
					mean		22.2	25.6	
					std		2.3	0.6	
JOHa-5	L5	$\phi 250$	300	0.60	1		28.8	44.6[1]	lb,rt
					2		38.8	38.8[1]	lb,rt
					mean		33.8	41.7	
					std		7.1	4.1	
JOHa-6	L6	$\phi 125$	300	0.60	1		-[2]	40.2[1]	lb,rt
					2		-[2]	40.0[1]	lb,rt
					mean		-	40.1	
					std		-	0.1	
Test series notation	Original test notation	Hole design ϕ or $a \times b,\ r$ [mm]	l [mm]	$\frac{M}{VH}$ [-]	i	M_{c0} [kNm]	M_c [kNm]	M_f [kNm]	LoC
JOHb-1	L5-3	$\phi 250$	2500	∞	1		114.0	122.7[1]	lt,rt

[1] = Maximum load.
[2] = No cracks.

2.5.2 Paper II

Paper II is titled *On the Design of Glued Laminated Timber Beams with Holes* [16] and deals with prior test performed by Dahl and Bengtsson, Kolb and Frech and the tests from Paper I. These tests are in this report presented in Sections 2.2, 2.3 and 2.5.1.

2.5.3 Paper III

Paper III, *Tests on Two Glued Laminated Timber Beams* [17], deals with the testing of two different beams. One beam, denoted Beam 1 in the original source, was first subjected to dead-weight loading for 2 days and strains at various positions were measured. The beam was after that loaded by a single point load of 30 kN at midspan and strains were recorded during a time period of two months. A short term test was thereafter performed. The other of the two beams, denoted Beam 2 in the original source, was only tested in short term loading. The tests on Beam 1 are excluded from this compilation and the following sections hence only concern Beam 2.

Material

The tested beam was delivered by *Töreboda Limträ AB* and made of Swedish spruce (Lat. *Picea Abies*). It was of strength class L40 and glued with a phenol-resorcinol glue with a lamellae thickness of 33 mm. Special attention was not given to climate conditioning of the beam. Since it was kept in a dry laboratory hall, the moisture content was believed to be 8-10 % but this was not controlled by measurements.

Test Setup

The beam was tested in a three-point-bending test according to Figure 2.1 and the beam geometry is presented in Table 2.12. The hole was rectangular and the corners of the hole were rounded with a radius of 25 mm.

Table 2.12: *Beam geometry and test setup, Johannesson III, 1983.*

Beam series	Test setup	n	L_{tot} [mm]	L [mm]	$H \times T$ [mm^2]	c [mm]	d [mm]	e [mm]	f [mm]	g_P [mm]	g_S [mm]
JOHc	1	1	4000	3800	400×140	1900	1900	-	-	?	?

Results

The hole design and the result of this test are presented in Table 2.13. It is in the original source stated that the beam was "severely cracked" at the hole at a load of 30 kN which here is considered as V_c. The load was thereafter increased to 37 kN before unloading but whether the reason for unloading was failure is unclear.

Table 2.13: *Hole design and test results, Johannesson III, 1983.*

Test series notation	Original test notation	Hole design ϕ or $a \times b,\ r$ [mm]	l [mm]	$\frac{M}{VH}$ [-]	i	V_{c0} [kN]	V_c [kN]	V_f [kN]	LoC
JOHc-1	Beam 2	$600 \times 200,\ 25$	900	1.58	1		30	37[1]	lb

[1] = Maximum load.

2.5.4 Paper IV

Paper IV, *Spänningsberäkning av anisotropa skivor* (Stress calculation of anisotropic plates) [18], deals with theory concerning calculation methods.

2.5.5 Paper V

This paper, *Limträbalkar med hål* (Glulam beams with holes) [19], holds the most extensive of Johannesson's beam series with a total of 30 separate tests.

Material

The beams used for the tests presented in Paper V were supplied by two separate Swedish producers, *Töreboda Limträ AB* and *Martinsons Trävaru AB*. They were all of strength class L40, made of Swedish spruce (Lat. *Picea Abies*) and glued with a phenol-resorcinol glue. The moisture content of the beams at testing was 11-15 %.

Test setup

The tests were performed on 16 glulam beams with circular or rectangular holes. In 14 out of the 16 beams, circular or rectangular holes were made at a distance of 1/4 of the span length L from each support. The second hole was made after testing the first hole for each beam. When testing the second hole, the beam was reinforced at the first hole using a steel box. Since these holes were placed at a distance from the supports of 1/4 of the span length, they were placed in a region subjected to both shear forces and bending moment. Notations and test setup for these 14 beams are shown in Figure 2.1. For the remaining two beams, a hole was placed at midspan where the beams were subjected to (almost) pure bending moment achieved by one point load on each side of the hole, according to Figure 2.2. This test arrangement thus results in a total of 30 separate tests according to Table 2.14. The corners of the rectangular holes were rounded with a radius of 25 mm and all hole surfaces were smoothed with sandpaper.

Table 2.14: *Beam geometry and test setup, Johannesson V, 1983.*

Beam series	Test setup	n	L_{tot} [mm]	L [mm]	$H \times T$ [mm^2]	c [mm]	d [mm]	e [mm]	f [mm]	g_P [mm]	g_S [mm]
JOHd	1	28	?	5000	495×88	2500	2500	-	-	?	?
JOHe	2	2	?	5000	495×88	1500	1500	2000	-	?	?

Results

The hole designs and the results of the tests from Paper V are presented in Tables 2.15 and 2.16. The definition of the crack load used by Johannesson for these tests is the same as the definition of V_c used in this compilation.

Table 2.15: *Hole design and test results (JOHd), Johannesson V, 1983.*

Test series notation	Original test notation	Hole design ϕ or $a \times b,\ r$ [mm]	l [mm]	$\frac{M}{VH}$ [-]	i	V_{c0} [kN]	V_c [kN]	V_f [kN]	LoC
JOHd-1	T2H2	$\phi 125$	1250	2.53	1		46.9		lb,rt
	T7H2				2		56.4		rt
	M2H2				3		>55.2		rt
	M7H2				4		49.2		rt,m
					mean		51.9		
					std		4.6		
JOHd-2	T1H1	$\phi 396$	1250	2.53	1		17.7		rt
	T5H2				2		16.6		lb,rt
	M1H1				3		14.2		lb,rt
	M5H2				4		16.0		lb,rt
					mean		16.1		
					std		1.5		
JOHd-3	T4H2	$125 \times 125,\ 25$	1250	2.53	1		24.4		lb,rt
	T6H2				2		45.0		lb,rt
	M4H2				3		50.0		lb,rt
	M6H2				4		42.0		lb
					mean		40.4		
					std		11.1		
JOHd-4	T4H1	$375 \times 125,\ 25$	1250	2.53	1		47.2		lb,rt
	T7H1				2		35.2		lb,rt
	M4H1				3		33.2		lb,rt
	M7H1				4		35.0		rt
					mean		37.7		
					std		6.4		
JOHd-5	T1H2	$370 \times 370,\ 25$	1250	2.53	1		9.0		rt
	T3H2				2		6.3		rt
	M1H2				3		9.8		lb
	M3H2				4		11.2		lb,rt
					mean		9.1		
					std		2.1		
JOHd-6	T2H1	$735 \times 245,\ 25$	1250	2.53	1		11.7		lb,rt
	T6H1				2		13.5		lb,rt
	M2H1				3		13.4		lb,rt
	M6H1				4		11.4		lb,rt
					mean		12.5		
					std		1.1		
JOHd-7	T3H1	$1110 \times 370,\ 25$	1250	2.53	1		4.5		rt
	T5H1				2		3.8		rt
	M3H1				3		4.0		rt
	M5H1				4		4.4		lb
					mean		4.2		
					std		0.3		

T = Töreboda, M = Martinsons.

Table 2.16: *Hole design and test results (JOHe), Johannesson V, 1983.*

Test series notation	Original test notation	Hole design ϕ or $a \times b,\ r$ [mm]	l [mm]	$\frac{M}{VH}$ [-]	i	M_{c0} [kNm]	M_c [kNm]	M_f [kNm]	LoC
JOHe-1	T8	$1110 \times 370,\ 25$	2500	∞	1		38.6		lt,rt
JOHe-2	M8	$\phi 396$	2500	∞	1		50.0		lt,rt

T = Töreboda, M = Martinsons.

2.6 Pizio, 1991

Pizio has performed tests on glulam beams with rectangular holes and these are reported in *Die Anwendung der Bruchmechanik zur Bemessung von Holzbauteilen, untersucht am durchbrochen und am ausgeklinkten Träger* (The use of fracture mechanics in design of timber structures, analysed on beams with holes and notched beams) [23] from 1991. Some beams were reinforced with bolts in the vicinity of the holes but these beams are however not included in this compilation.

Material

The beams were all of strength class B (Ger. *Klasse B*) according to the Swiss timber code SIA. The moisture content at the time of testing was 10-14 % for all beams.

Test setup

The beams were subjected to a three-point-bending test according to Figure 2.1. The geometry and test setups for the unreiforced beams included in this compilation are presented in Table 2.17. All rectangular holes seem to have had sharp corners.

Table 2.17: *Beam geometry and test setup, Pizio, 1991.*

Beam series	Test setup	n	L_{tot} [mm]	L [mm]	$H \times T$ [mm^2]	c [mm]	d [mm]	e [mm]	f [mm]	g_P [mm]	g_S [mm]
PIZa	1	6	1800	1620	400×120	910	710	-	-	250	180
PIZb	1	1	2000	1820	400×120	910	910	-	-	250	180
PIZc	1	1	2500	2320	400×120	910	1410	-	-	250	180
PIZd	1	3	2300	2120	400×120	1410	710	-	-	250	180
PIZe	1	6	2500	2320	400×120	1410	910	-	-	250	180
PIZf	1	2	2000	1420	400×120	910	510	-	-	250	180

Results

The hole designs and the results of the tests are presented in Table 2.18. Pizio defined and recorded three load levels when analysing the tests; the shear force at crack initiation, the shear force at a sudden and significant crack propagation and the maximum shear force. These three load levels are here assumed to correspond to V_{c0}, V_c and V_f respectively.

Table 2.18: *Hole design and test results, Pizio, 1991.*

Test series notation	Original test notation	Hole design ϕ or $a \times b,\ r$ [mm]	l [mm]	$\frac{M}{VH}$ [-]	i	V_{c0} [kN]	V_c [kN]	V_f [kN]	LoC
PIZa-1	TR1	$180 \times 180,\ 0$	420	1.05	1	15.3	28.4	60.4	lb,rt
	TR1A				2	32.8	32.8	66.9	lb,rt
					mean	24.1	30.6	63.7	
					std	12.4	3.1	4.6	
PIZa-2	TR2	$180 \times 90,\ 0$	420	1.05	1	26.3	52.5	76.6	rt
	TR2A				2	48.1	57.3	74.4	rt
					mean	37.2	54.9	75.5	
					std	15.4	3.4	1.6	
PIZa-3	TR3	$180 \times 10,\ 0$	420	1.05	1	113.8	113.8	113.8	lb,rt
	TR3A				2	76.6	92.8	92.8	lb,rt
					mean	95.2	103.3	103.3	
					std	26.3	14.8	14.8	
PIZb-1	TR2B	$180 \times 90,\ 0$	420	1.05	1	56.6	71.0	84.5	lb,rt
PIZc-1	TR3B	$180 \times 10,\ 0$	420	1.05	1	110.1	110.1	110.1	lb,rt
PIZd-1	TR8	$360 \times 180,\ 0$	700	1.75	1	20.0	23.3	26.3	lb,rt
	TR8A				2	23.3	23.3	23.3	lb,rt
					mean	21.7	23.3	24.8	
					std	2.3	0	2.1	
PIZd-2	TR9	$10 \times 180,\ 0$	700	1.75	1	34.0	34.0	34.0	lb,rt
PIZe-1	TR8B	$360 \times 180,\ 0$	700	1.75	1	19.2	21.1	28.8	lb,rt
PIZe-2	TR9A	$10 \times 180,\ 0$	700	1.75	1	29.2	33.8	33.8	lb,rt
	TR9B				2	30.8	33.8	33.8	lb,rt
					mean	30.0	33.8	33.8	
					std	1.1	0	0	
PIZe-3	TR11	$180 \times 90,\ 0$	700	1.75	1	44.2	46.2	46.2	lb,rt
	TR11A				2	35.4	58.8	58.8	lb,rt
	TR11B				3	57.7	57.7	57.7	lb,rt
					mean	45.8	54.2	54.2	
					std	11.2	7.0	7.0	
PIZf-1	TR 4	$180 \times 180,\ 0$	420	1.05	1	24.1	29.5	62.1	lb,rt
	TR 4A				2	17.1	24.1	77.9	lb,rt
					mean	20.6	26.8	70.0	
					std	4.9	3.8	11.2	

2.7 Hallström, 1995

Hallström's reports *Glass fibre reinforcemed laminated timber beams with holes* [8] and *Glass fibre reinforcement around holes in laminated timber beams* [9] from 1995 deal with investigations on reinforcement of glulam beams with circular or rectangular holes by glass fibre. Tests were carried out on both reinforced holes and unreiforced holes and the latter are included in this compilation.

Material

The glulam beams used for the tests were made of Swedish spruce (Lat. *Picea Abies*) and glued with phenol-resorcinol resin glue. No special attention was given to climate conditioning of the beams but since they were kept at normal indoor climate for a month prior to testing, the moisture content was assumed to be 6-13 %. The density of the beams varied between 350-550 kg/m^3.

Test setup

The tests were all performed as three-point-bending test according to Figure 2.1 where the holes were all placed in a region subjected to both shear force and bending moment. The geometries of the beams are presented in Table 2.19. For beams with rectangular holes, both rounded and sharp corners were tested.

Table 2.19: *Beam geometry and test setup, Hallström, 1995.*

Beam series	Test setup	n	L_{tot} [mm]	L [mm]	$H \times T$ [mm^2]	c [mm]	d [mm]	e [mm]	f [mm]	g_P [mm]	g_S [mm]
HALa	1	15	4500	4000	315×90	2000	2000	-	-	340	170
HALb	1	5	3500	3000	315×90	1500	1500	-	-	340	170
HALc	1	1	3500	3000	315×90	1500	1500	-	-	?	?
HALd	1	4	7000	6000	585×165	3000	3000	-	-	?	?

Results

Hallström defined the "failure load" as the maximum load before the first visible load decrease in the load-deflection curve. This decrease in the load-deflection curve is most likely due to crack opening in the entire beam width and Hallström's "failure loads" are thus considered correspond to the definition of V_c used in this report. Only mean values and standard deviations are presented in Table 2.20 since the results for the individual tests are not to be found in [8] or [9].

Table 2.20: *Hole design and test results, Hallström, 1995.*

Test series notation	Original test notation	Hole design ϕ or $a \times b,\ r$ [mm]	l [mm]	$\frac{M}{VH}$ [-]	i	V_{c0} [kN]	V_c [kN]	V_f [kN]	LoC
HALa-1	-	$400 \times 150,\ 25$	875	2.78	1		?		
					2		?		
					3		?		
					4		?		
					5		?		
					mean		11.9		lb,rt
					std		1.5		
HALa-2	-	$400 \times 150,\ 0$	875	2.78	1		?		
					2		?		
					3		?		
					4		?		
					5		?		
					mean		12.2		lb,rt
					std		1.1		
HALa-3	-	$\phi 150$	875	2.78	1		?		
					2		?		
					3		?		
					4		?		
					5		?		
					mean		24.5		lb,rt
					std		3.5		
HALb-1	-	$400 \times 150,\ 25$	875	2.78	1		?		
					2		?		
					3		?		
					4		?		
					5		?		
					mean		12.2		lb,rt
					std		0.5		
HALc-1	-	$400 \times 150,\ 25$	?	?	1		12.2		lb,rt
HALd-1	-	$600 \times 295,\ 25$	?	?	1		?		
					2		?		
					3		?		
					4		?		
					mean		27.1		lb,rt
					std		1.9		

2.8 Höfflin, 2005

Höfflin's doctoral thesis *Runde Durchbrüche in Brettschichtholzträger – Experimentelle und theoretische Untersuchungen* (Round holes in glulam beams – Experimental and theoretical analyses) [12] from 2005 deals with the capacity of glulam beams with round holes and includes extensive experimental testing on different beam and hole geometries.

Material

All tested beams were made of spruce (Ger. *fichte*) with a mean density of 488 kg/m^3 and of strength class GL32h (BS 16h). No special attention was given to knots, cracks or other minor defects when placing the holes. The lamellae thickness was 40 mm or 32 mm and the moisture content at the time of testing was 10.4±1.5 %.

Test setup

Four different beam geometries and test setups were used in order to achieve the desired ratio of cross sectional forces at the holes. The used test setups are presented in Figures 2.1, 2.2 and 2.3 while the used beam geometries are found in Table 2.21.

Table 2.21: *Beam geometry and test setup, Höfflin, 2005.*

Beam series	Test setup	n	L_{tot} [mm]	L [mm]	$H \times T$ [mm^2]	c [mm]	d [mm]	e [mm]	f [mm]	g_P [mm]	g_S [mm]
HOFa	1	15	3375	3150	450 × 120	1575	1575	-	-	300	225
HOFb	2	17	6750	6300	900 × 120	2700	2700	900	-	450	450
HOFc	3	5	5045	4675	450 × 120	788	788	400	1350	225	370
HOFd	3	5	9950	9450	900 × 120	1575	1575	900	2700	450	500

Results

The hole designs and the results of the tests are presented in Tables 2.22 and 2.23. The definitions of the different load levels used by Höfflin correspond well to the definitions of V_{c0}, V_c and V_f used in this compilation. The loads for crack initiation and crack propagation across the entire beam width are in [12] presented separately for the different corners. For some beams, cracks open up simultaneously while the cracks open up at different load levels for other beams. For the cases when cracks did not open up simultaneously in two corners of the hole, the lower of the two values are used in this compilation.

Table 2.22: *Hole design and test results (HOFa and HOFb), Höfflin, 2005.*

Test series notation	Original test notation	Hole design ϕ or $a \times b$, r [mm]	l [mm]	$\frac{M}{VH}$ [-]	i	V_{c0} [kN]	V_c [kN]	V_f [kN]	LoC
HOFa-1	450_ 1.5h_0.2	ϕ90	675	1.50	1	82.5	85.5	85.5	lb,rt
					2	77.0	91.1	91.1	lb,rt
					3	51.0	74.6	74.6	lb,rt
					4	53.5	77.6	85.4	lb,rt
					5	50.2	55.1	73.8	lb,rt
					mean	62.8	76.8	82.1	
					std	15.6	13.8	7.6	
HOFa-2	450_ 1.5h_0.3	ϕ135	675	1.50	1	41.0	52.5	59.3	lb,rt
					2	45.2	75.0	75.0	lb,rt
					3	38.1	69.4	77.2	lb,rt
					4	62.6[1]	62.6	62.6	lb,rt
					5	66.7[1]	66.7	66.7	lb,rt
					6	30.9	66.5	66.5	lb,rt
					mean	47.4	65.5	67.9	
					std	14.2	7.6	7.0	
HOFa-3	450_ 1.5h_0.4	ϕ180	675	1.50	1	30.3	38.3	44.5	lb,rt
					2	27.0	45.0	53.4	lb,rt
					3	38.0	48.3	50.6	lb,rt
					4	43.3	58.7	58.7	lb,rt
					mean	34.6	47.6	51.8	
					std	7.4	8.5	5.9	
HOFb-1	900_ 1.5h_0.2	ϕ180	1350	1.50	1	62.5	88.0	119.2	lb,rt
					2	66.6	86.1	110.0	lb,rt
					3	53.0	90.0	114.2	lb,rt
					4	109.5	117.0	144.8	lb,rt
					5	54.3	150.7	152.5	lb,rt
					mean	69.2	106.4	128.1	
					std	23.2	27.8	19.2	
HOFb-2	900_ 1.5h_0.3	ϕ270	1350	1.50	1	78.8	96.0	115.8	lb,rt
					2	55.1	112.0	116.0	lb,rt
					3	66.4	90.5	100.9	lb,rt
					4	26.4	81.0	102.6	lb,rt
					5	76.9	90.9	104.9	lb,rt
					6	88.0	108.2	112.1	lb,rt
					mean	65.3	96.4	108.7	
					std	22.1	11.7	6.7	
HOFb-3	900_ 1.5h_0.4	ϕ360	1350	1.50	1	-[2]	-[2]	81.9	lb,rt
					2	52.0	67.5	72.4	lb,rt
					3	84.0[1]	84.0	117.3	lb,rt
					4	60.0[1]	60.0	85.4	lb,rt
					5	38.3	69.0	79.3	lb,rt
					6	53.6	65.3	88.8	lb,rt
					mean	57.6	69.2	87.5	
					std	16.8	9.0	15.6	

[1] = Not included in [12] but found in [2].
[2] = V_{c0} and V_c not recorded for this test.

Table 2.23: *Hole design and test results (HOFc and HOFd), Höfflin, 2005.*

Test series notation	Original test notation	Hole design ϕ or $a \times b,\ r$ [mm]	l [mm]	$\frac{M}{VH}$ [-]	i	V_{c0} [kN]	V_c [kN]	V_f [kN]	LoC
HOFc-1	450_ 5h_0.3	ϕ135	1463	5.00	1	42.0	58.5	58.5	lb,rt
					2	59.8	70.0	70.0	lb,rt
					3	12.7	52.4	68.1	lb,rt
					4	36.9	54.8	54.8	lb,rt
					5	22.1	54.1	65.6	lb,rt
					mean	34.7	58.0	63.4	
					std	18.2	7.1	6.5	
HOFd-1	900_ 5h_0.3	ϕ270	2925	5.00	1	35.5	48.0	95.6	lb,rt
					2	46.3	50.9	74.1	lb,rt
					3	38.0	50.0	93.8	lb,rt
					4	39.5	69.2	100.1	lb,rt
					5	56.0	57.5	57.5	lb,rt
					mean	43.1	55.1	84.2	
					std	8.3	8.6	18.0	

2.9 Aicher and Höfflin, 2006

In the rapport *Tragfähigkeit und Bemessung von Brettschichtholzträgern mit runden Durchbrüchen – Sicherheitsrelevante Modifikationen der Bemessungsverfahren nach Eurocode 5 und DIN 1052* (Load capacity and design of glulam beams with round holes – Safety relevant modifications of design methods according to Eurocode 5 and DIN 1052) [2] from 2006 the tests presented in [12] (Section 2.8) and some additional tests are presented. These additional tests consists of 15 tests on straight glulam beams and six tests on curved glulam beams with holes.

Material

The beams used in these tests were all of quality class GL 32h (BS 16h) and made of spruce (Ger. *fichte*). No special attention was given to knots or other defects when placing the holes. The moisture content in the beams at the time of testing was 10.9±1.5 %. The density at a moisture content of 12 % was 471±38 kg/m^3.

Test setup

Beam series AICa and AICb consist of straight beams which were tested using test setup 3 according to Figure 2.3. Beam series AICc and AICd consist of curved beams with $H/r_m = 0.03$ which means that the curvature radius $r_m = 15$ m for beam series AICc and $r_m = 30$ m for beam series AICd. The test setups for these beam series are presented in Figures 2.4 and 2.5. The beam geometries for the four beam series are presented in Table 2.24.

Table 2.24: *Beam geometry and test setup, Aicher and Höfflin, 2006.*

Beam series	Test setup	n	L_{tot} [mm]	L [mm]	$H \times T$ [mm^2]	c [mm]	d [mm]	e [mm]	f [mm]	g_P [mm]	g_S [mm]
AICa	3	6	5045	4675	450 × 120	788	788	400	1350	225	370
AICb	3	9	9950	9450	900 × 120	1575	1575	900	2700	450	500
AICc	4	3	4725	4500	450 × 120	2925	1575	-	-	360	250
AICd	5	3	9450	9000	900 × 120	5850	2150	1000	-	600	450

Results

The hole designs and the results of the tests are presented in Tables 2.25. The same definitions of the different load levels are used in this report as in [12] and these definitions correspond well with the definitions used in this compilation. The loads for crack initiation and crack propagation across the entire beam width are in [2] presented separately for the different corners. For some beams, cracks open up simultaneously while the cracks open up at different load levels for other beams. For the cases when cracks did not open up simultaneously in two corners of the hole, the lower of the two values are used in this compilation.

Table 2.25: *Hole design and test results, Aicher and Höfflin, 2006.*

Test series notation	Original test notation	Hole design ϕ or $a \times b,\ r$ [mm]	l [mm]	$\frac{M}{VH}$ [-]	i	V_{c0} [kN]	V_c [kN]	V_f [kN]	LoC
AICa-1	450_ 5h_0.4	ϕ180	1263	5.00	1	45.8	50.0	61.0	lb,rt
					2	57.8	63.5	63.5	lb,rt
					3	40.1	43.8	44.0	lb,rt
					4	35.8	46.7	48.0	lb,rt
					5	45.0	46.7	57.5	lb,rt
					6	29.8	42.0	48.0	lb,rt
					mean	42.4	48.8	53.7	
					std	9.6	7.7	8.0	
AICb-1	900_ 5h_0.2	ϕ180	2925	5.00	1	62.7	107.1	107.1	rt
					2	-	101.4	101.4	?
					3	89.5	126.4	126.4	rt
					4	47.0	90.6	-[1]	lb,rt
					mean	66.4	106.4	111.6	
					std	21.5	15.0	13.1	
AICb-2	900_ 5h_0.4	ϕ360	2925	5.00	1	60.8	62.6	82.7	lb,rt
					2	62.0	77.2	77.2	lb,rt
					3	42.5	68.5	82.7	lb,rt
					4	43.0	62.5	-[1]	lb,rt
					5	25.0	37.0	77.0	lb,rt
					mean	46.7	61.6	79.9	
					std	15.3	15.0	3.2	
AICc-1	G450_ 5h_0.4	ϕ180	2250	5.00	1	14.7	44.5	46.9	lb,rt
					2	18.7	38.4	45.5	lb,rt
					3	12.7	30.9	42.0	lb,rt
					mean	15.4	37.9	44.8	
					std	3.1	6.8	2.5	
AICd-1	G900_ 5h_0.4	ϕ360	4500	5.00	1	18.0	36.0	71.9	lb,rt
					2	43.7	43.7	58.8	lb,rt
					3	38.8	69.2	69.2	rt
					mean	33.5	49.6	66.6	
					std	13.6	17.4	6.9	

[1] = Value not included in [2] since failure was partially or completely caused by bending.

2.10 Summary of experimental tests

A summary of the beam series are presented in Table 2.26. The test results for holes place in shear force dominated region are presented in Table 2.27 and Figure 2.8 for circular holes and in Table 2.28 and Figure 2.9 for rectangular holes. The test results for holes placed in a pure moment region are presented in Table 2.29 and Figure 2.10. The hole design are in these figures represented by the ratio D/H where H is the beam height and $D = \phi$ for circular holes and $D = \sqrt{a^2 + b^2}$ for rectangular holes. The test results for beams with holes in shear force dominated region are presented as mean shear stress V/A_{net} where A_{net} is the net cross section area according to Equation (2.1) for circular holes and Equation (2.2) for rectangular holes. For beams with holes in pure moment region, the bending moment M is normalized with respect to the elastic section modulus of the net cross section W_{net} according to Equation (2.3). Comments on whether the definitions of the different load levels from the original source correspond well or not with the definitions used in this report are not stated here but found in the previous sections on this chapter.

Table 2.26: *Summary of beam series.*

Beam series	Test setup	n	L_{tot} [mm]	L [mm]	$H \times T$ [mm^2]	c [mm]	d [mm]	e [mm]	f [mm]	g_P [mm]	g_S [mm]
BEN	1	7	5300	5000	500×90	2500	2500	-	-	?	?
FRE	2	12	8400	8000	550×80	2000	2000	4000	-	?	?
PENa	1	6	4300	4000	500×90	2000	2000	-	-	?	?
PENb	1	4	5400	5000	800×115	2500	2500	-	-	?	?
JOHa	1	12	-	5000	500×90	2500	2500	-	-	?	?
JOHb	2	1	-	5000	500×90	2000	2000	1000	-	?	?
JOHc	1	1	4000	3800	400×140	1900	1900	-	-	?	?
JOHd	1	28	?	5000	495×88	2500	2500	-	-	?	?
JOHe	2	2	?	5000	495×88	1500	1500	2000	-	?	?
PIZa	1	6	1800	1620	400×120	910	710	-	-	250	180
PIZb	1	1	2000	1820	400×120	910	910	-	-	250	180
PIZc	1	1	2500	2320	400×120	910	1410	-	-	250	180
PIZd	1	3	2300	2120	400×120	1410	710	-	-	250	180
PIZe	1	6	2500	2320	400×120	1410	910	-	-	250	180
PIZf	1	2	2000	1420	400×120	910	510	-	-	250	180
HALa	1	15	4500	4000	315×90	2000	2000	-	-	340	170
HALb	1	5	3500	3000	315×90	1500	1500	-	-	340	170
HALc	1	1	3500	3000	315×90	1500	1500	-	-	?	?
HALd	1	4	7000	6000	585×165	3000	3000	-	-	?	?
HOFa	1	15	3375	3150	450×120	1575	1575	-	-	300	225
HOFb	2	17	6750	6300	900×120	2700	2700	900	-	450	450
HOFc	3	5	5045	4675	450×120	788	788	400	1350	225	370
HOFd	3	5	9950	9450	900×120	1575	1575	900	2700	450	500
AICa	3	6	5045	4675	450×120	788	788	400	1350	225	370
AICb	3	9	9950	9450	900×120	1575	1575	900	2700	450	500
AICc	4	3	4725	4500	450×120	2925	1575	-	-	360	250
AICd	5	3	9450	9000	900×120	5850	2150	1000	-	600	450

Table 2.27: *Summary of test results for beams with circular holes in shear force dominated region.*

Test series notation	Hole design ϕ [mm]	$\frac{M}{VH}$ [-]	n	V_{c0} Mean [kN]	V_{c0} (Std) [kN]	V_c Mean [kN]	V_c (Std) [kN]	V_f Mean [kN]	V_f (Std) [kN]
BEN-1	ϕ250	1.20	2					38.4	(1.2)
BEN-3	ϕ150	1.20	1					52.5	
PENa-1	ϕ255	1.20	1					33.8	
PENa-2	ϕ250	2.10	1					31.6	
PENa-3	ϕ150	1.20	1					51.3	
PENb-1	ϕ400	1.03	1	57.1				65.9	
PENb-2	ϕ300	2.00	1					89.5	
JOHa-1	ϕ250	1.30	2			29.6	(5.4)	36.5	(4.3)
JOHa-3	ϕ250	2.80	2			33.2	(2.6)	37.5	(3.5)
JOHa-5	ϕ250	0.60	2			33.8	(7.1)	41.7	(4.1)
JOHa-6	ϕ125	0.60	2			-		40.1	(0.1)
JOHd-1	ϕ125	2.53	4			51.9	(4.6)		
JOHd-2	ϕ396	2.53	4			16.1	(1.5)		
HALa-3	ϕ150	2.78	5			24.5	(3.5)		
HOFa-1	ϕ90	1.50	5	62.8	(15.6)	76.8	(13.8)	82.1	(7.6)
HOFa-2	ϕ135	1.50	6	38.8	(6.0)	65.5	(7.6)	67.9	(7.0)
HOFa-3	ϕ180	1.50	4	34.6	(7.4)	47.6	(8.5)	51.8	(5.9)
HOFb-1	ϕ180	1.50	5	69.2	(23.2)	106.4	(27.8)	128.1	(19.2)
HOFb-2	ϕ270	1.50	6	65.3	(22.1)	96.4	(11.7)	108.7	(6.7)
HOFb-3	ϕ360	1.50	6	48.0	(8.4)	69.2	(9.0)	87.5	(15.6)
HOFc-1	ϕ135	5.00	5	34.7	(18.2)	58.0	(7.1)	63.4	(6.5)
HOFd-1	ϕ270	5.00	5	43.1	(8.3)	55.1	(8.6)	84.2	(18.0)
AICa-1	ϕ180	5.00	6	42.4	(9.6)	48.8	(7.7)	53.7	(8.0)
AICb-1	ϕ180	5.00	4	66.4	(21.5)	106.4	(15.0)	111.6	(13.1)
AICb-2	ϕ360	5.00	5	46.7	(15.3)	61.6	(15.0)	79.9	(3.2)
AICc-1	ϕ180	5.00	3	15.4	(3.1)	37.9	(6.8)	44.8	(2.5)
AICd-1	ϕ360	5.00	3	33.5	(13.6)	49.6	(17.4)	66.6	(6.9)

$$A_{net} = T(H - \phi) \tag{2.1}$$

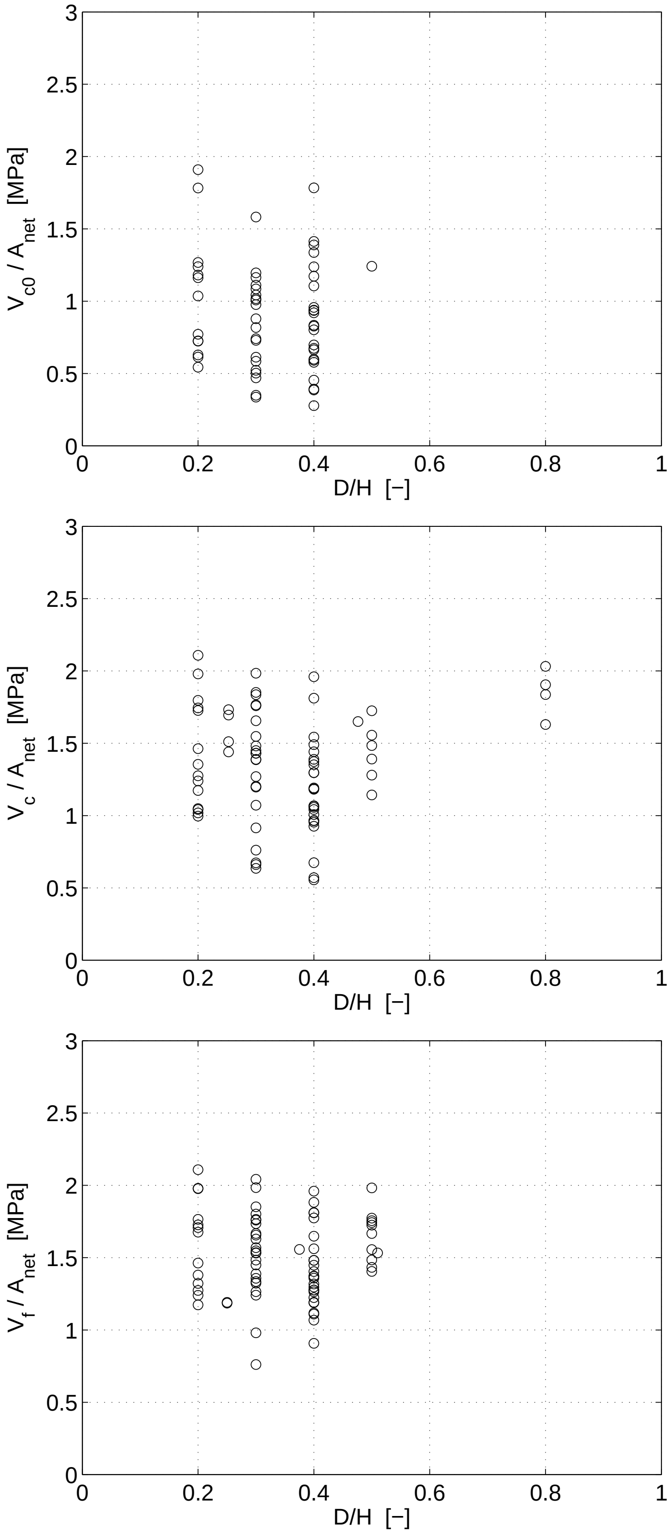

Figure 2.8: *Mean shear stress* V/A_{net} *for load levels* V_{c0} *(top),* V_c *(middle) and* V_f *(bottom) for circular holes in shear force dominated region.* $D = \phi$.

Table 2.28: *Summary of test results for beams with rectangular holes in shear force dominated region.*

Test series notation	Hole design $a \times b$ [mm^2]	r [mm]	$\frac{M}{VH}$ [-]	n	V_{c0} Mean [kN]	V_{c0} (Std) [kN]	V_c Mean [kN]	V_c (Std) [kN]	V_f Mean [kN]	V_f (Std) [kN]
BEN-2	300 × 150	0	1.20	2					39.0	(0.3)
BEN-4	200 × 100	0	1.20	2					49.6	(1.1)
FRE-1	250 × 250	?	0.91	2					32.7	(2.1)
FRE-2	250 × 150	?	0.91	2					44.0	(2.8)
FRE-3	250 × 250	?	1.82	2					33.8	(1.1)
FRE-4	250 × 150	?	1.82	2					35.4	(4.0)
PENa-4	200 × 200	?	1.60	1					33.8	
PENa-5	400 × 200	?	1.60	1	25.0				31.3	
PENa-6	600 × 200	?	1.60	1	20.8				30.0	
PENb-3	400 × 200	?	1.25	1					69.1	
PENb-4	200 × 200	?	1.25	1	52.5				84.4	
JOHa-2	250 × 250	25	1.30	2			26.8	(0.5)	28.5	(2.8)
JOHa-4	250 × 250	25	2.80	2			22.2	(2.3)	25.6	(0.6)
JOHc-1	600 × 200	25	2.25	1			30.0		37.0	
JOHd-3	125 × 125	25	2.53	4			40.4	(11.1)		
JOHd-4	375 × 125	25	2.53	4			37.7	(6.4)		
JOHd-5	370 × 370	25	2.53	4			9.1	(2.1)		
JOHd-6	735 × 245	25	2.53	4			12.5	(1.1)		
JOHd-7	1110 × 370	25	2.53	4			4.2	(0.3)		
PIZa-1	180 × 180	0	1.05	2	24.1	(12.4)	30.6	(3.1)	63.7	(4.6)
PIZa-2	180 × 90	0	1.05	2	37.2	(15.4)	54.9	(3.4)	75.5	(1.6)
PIZa-3	180 × 10	0	1.05	2	95.2	(26.3)	103.3	(14.8)	103.3	(14.8)
PIZb-1	180 × 90	0	1.05	1	56.6		71.0		84.5	
PIZc-1	180 × 10	0	1.05	1	110.1		110.1		110.1	
PIZd-1	360 × 180	0	1.75	2	21.7	(2.3)	23.3	(0.0)	24.8	(2.1)
PIZd-2	10 × 180	0	1.75	1	34.0		34.0		34.0	
PIZe-1	360 × 180	0	1.75	1	19.2		21.1		28.8	
PIZe-2	10 × 180	0	1.75	2	30.0	(1.1)	33.8	(0.0)	33.8	(0.0)
PIZe-3	180 × 90	0	1.75	3	45.8	(11.2)	54.2	(7.0)	54.2	(7.0)
PIZf-1	180 × 180	0	1.05	2	20.6	(4.9)	26.8	(3.8)	70.0	(11.2)
HALa-1	400 × 150	25	2.78	5			11.9	(1.5)		
HALa-2	400 × 150	0	2.78	5			12.2	(1.1)		
HALb-1	400 × 150	25	2.78	5			12.2	(0.5)		
HALc-1	400 × 150	25	?	1			12.2			
HALd-1	600 × 295	25	?	4			27.1	(1.9)		

$$A_{net} = T(H - b) \tag{2.2}$$

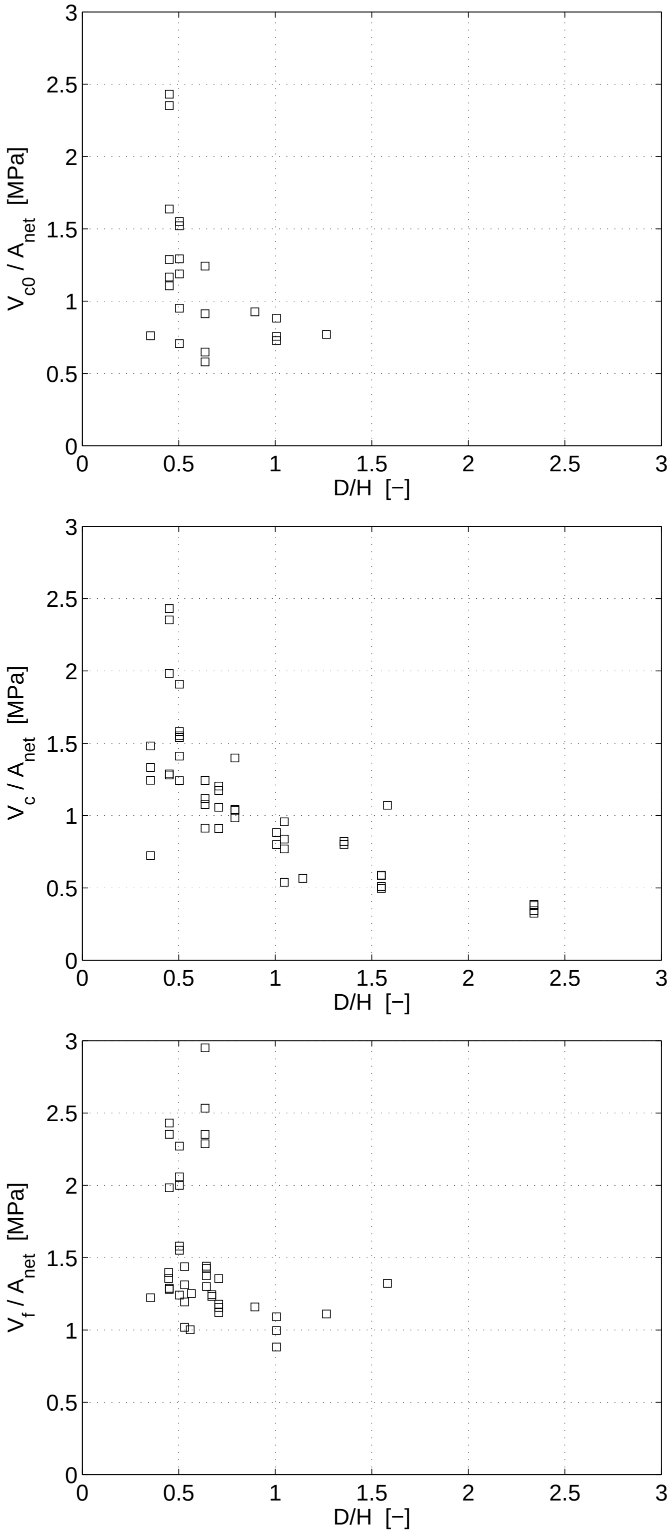

Figure 2.9: *Mean shear stress V/A_{net} for load levels V_{c0} (top), V_c (middle) and V_f (bottom) for rectangular holes in shear force dominated region.* $D = \sqrt{a^2 + b^2}$.

Table 2.29: *Summary of test results for beams with holes in pure moment region.*

Test series notation	Hole design ϕ or $a \times b,\ r$ [mm]	l [m]	$\frac{M}{VH}$ [-]	n	M_{c0} mean (std) [kNm]	M_c mean (std) [kNm]	M_f mean (std) [kNm]
FRE-5	$\phi 300$	4000	∞	2			140.0 (0.0)
FRE-6	$300 \times 300,\ ?$	4000	∞	2			136.8 (4.5)
JOHb-1	$\phi 250$	2500	∞	1		114.0	122.7
JOHe-1	$1110 \times 370,\ 25$	2500	∞	1		38.6	
JOHe-2	$\phi 396$	2500	∞	1		50.0	

$$W_{net} = \frac{T}{6H}(H^3 - x^3) \qquad x = b \text{ for rectangular holes and } \phi \text{ for circular holes} \quad (2.3)$$

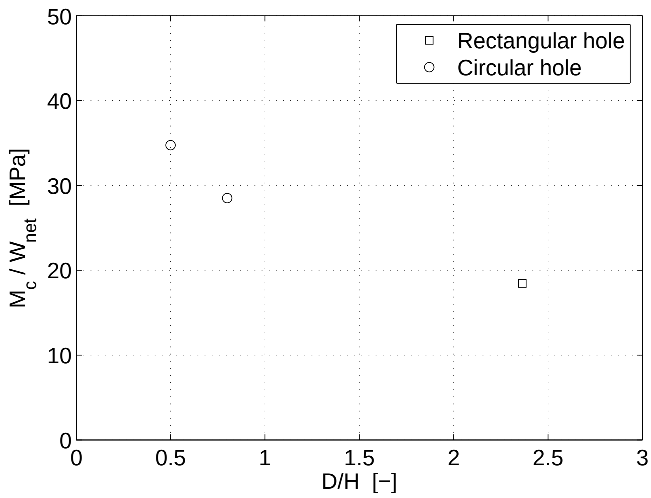

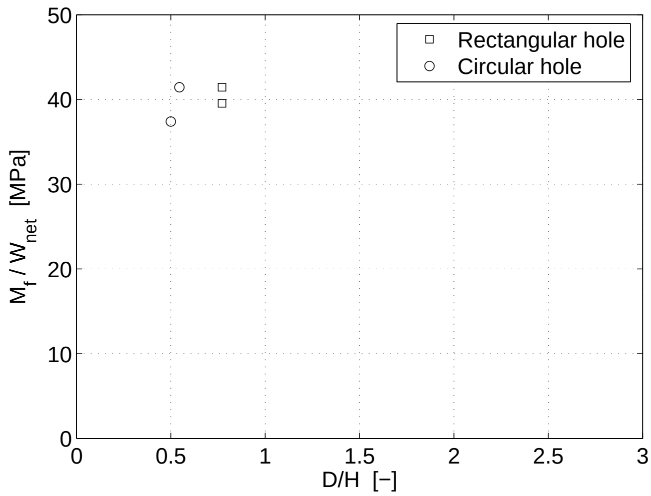

Figure 2.10: *M/W_{net} for load levels M_c (top) and M_f (bottom) for holes in pure moment region. $D = \phi$ or $\sqrt{a^2 + b^2}$.*

Chapter 3

Methods for theoretical strength analysis

There are several available methods for strength analysis when it comes to timber engineering. Timber is in many aspects a more complex construction material compared to for example steel. This is partly due to the anisotropic properties and the large differences in strength between loading modes. Assumptions and simplifications for a certain material model may be acceptable for some applications but may for other cases lead to unreliable results if the analysis is possible to perform at all.

A distinction can be made between deterministic and stochastic material models. In the deterministic models, wood is viewed as a homogeneous material with the same material properties in all points. In the stochastic models, the natural heterogeneity due to knots and other defects is considered by some type of statistical measure. Distinctions between different models can also be made based on whether the material is considered to be ideally brittle or if the material has fracture ductility. The various kind of rational methods for strength analysis of timber elements can be categorized as in Table 3.1. They are all more or less briefly described in this chapter.

Table 3.1: *Models for timber engineering strength analysis* [29].

	Deterministic (homogeneous)	**Stochastic** (heterogenous)
Brittle $G_f = 0$	Conventional stress analysis	Weibull weakest link theory
With fracture ductility $G_f \neq 0$	Linear elastic fracture mechanics Generalized linear elastic fracture mechanics Nonlinear fracture mechanics	Probabilistic fracture mechanics

3.1 Conventional stress analysis

The most common approach when designing timber structures is a conventional stress analysis with a stress-based failure criterion. The state of stresses is commonly determined at the assumption of a linear elastic material which is continuous, homogeneous, transversely isotropic and brittle with deterministic properties. This method is in many cases insufficient, since the assumptions are too inaccurate for many applications. Larger timber elements and wooden products such as glulam have heterogeneous properties due to knots, initial cracks and other defects which appear stochastically in the material. Assuming transversely isotropic and homogeneous material properties means that two simplifications are introduced. There is no distinction made between material properties in radial and tangential direction and the material directions and properties are assumed to be identical in the entire body. These simplifications may have a large impact on the results of a stress analysis since the material properties vary significantly with the orientation of the annual rings. Wood is further not ideally brittle. The fracture toughness also varies with the type of fracture (tension or compression, perpendicular or parallel to grain etc.). The differences between the material assumptions and reality is often treated by the use of correction factors and limitations based on equations derived from empirical observations. [29]

Failure criteria

In conventional stress analysis, failure is assumed to occur as soon as any point in the stressed body fulfills a certain criterion. A commonly used failure criterion for the case of a plane state of stress is Norris' criterion according to Equation (3.1) where σ_{90} and σ_0 are stresses perpendicular and parallel to grain respectively and τ is the shear stress. The material strengths f_{90} and f_0 are assigned different values for tensile or compressive stresses. The shear strength of the material is denoted f_v. Hence, five material parameters are here involved.

$$\left(\frac{\sigma_{90}}{f_{90}}\right)^2 + \left(\frac{\sigma_0}{f_0}\right)^2 + \left(\frac{\tau}{f_v}\right)^2 = 1 \tag{3.1}$$

Norris' criterion in three dimensions for an orthotropic material is stated in Equations (3.2), (3.3) and (3.4) where the indexes 1, 2 and 3 corresponds to the three material directions; longitudinal, radial and tangential.

$$\left(\frac{\sigma_1}{f_1}\right)^2 + \left(\frac{\sigma_2}{f_2}\right)^2 + \left(\frac{\tau_{12}}{f_{v12}}\right)^2 - \frac{\sigma_1\sigma_2}{f_1 f_2} = 1 \tag{3.2}$$

$$\left(\frac{\sigma_1}{f_1}\right)^2 + \left(\frac{\sigma_3}{f_3}\right)^2 + \left(\frac{\tau_{13}}{f_{v13}}\right)^2 - \frac{\sigma_1\sigma_3}{f_1 f_3} = 1 \tag{3.3}$$

$$\left(\frac{\sigma_3}{f_3}\right)^2 + \left(\frac{\sigma_2}{f_2}\right)^2 + \left(\frac{\tau_{32}}{f_{v32}}\right)^2 - \frac{\sigma_3\sigma_2}{f_3 f_2} = 1 \tag{3.4}$$

For the case of uniaxial loading at an angle α to grain, Hankinsons's expression according to Equation (3.5) is well used. The equation holds for both tensile and compressive stresses when the corresponding strength parameters are used. In literature, the value of n is commonly stated as 2.

$$\sigma_\alpha = \frac{f_{90} f_0}{f_{90} \cos^n \alpha + f_0 \sin^n \alpha} \tag{3.5}$$

Stress components can sometimes be considered separately yielding the following rather simple failure criteria for the case of plane stress.

$$\begin{cases} \sigma_{90} & = & f_{90} \\ \sigma_0 & = & f_0 \\ \tau & = & f_v \end{cases} \tag{3.6}$$

3.2 Linear elastic fracture mechanics – LEFM

Linear elastic fracture mechanics (LEFM) deals with analysis of cracks and propagation of cracks. The theory is based on the assumption of an ideally linear elastic behaviour of the material and the existence of a crack (or a sharp notch). Although stresses and strains may be very large in the vicinity of the tip of the crack, the theory of small strains is used. LEFM can not be used to determine where one can expect a crack in a stressed body to arise but it can be used for analysis of whether an existing crack will propagate or not. Crack propagations analysis can be done by considering the energy balance of the system, by considering the so called stress intensity factors or by some other similar method.

A consequence of the assumption of an ideally linear elastic material is that stresses at the tip of a crack theoretically are infinite, see Figure 3.1. This rules out the use of a stress-based failure criterion but is however accepted in LEFM as long as the fracture process region, i.e. the area exposed to large stresses, is small compared to the length of the crack and also compared to the distance to loads and supports. For wood, the fracture process region is approximately one to a few centimeters.

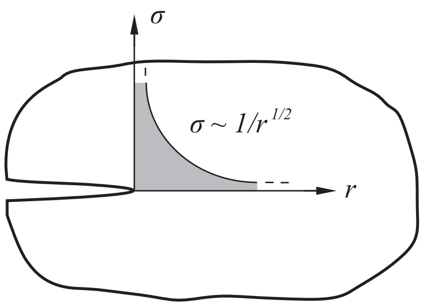

Figure 3.1: *Linear elastic stress distribution at the tip of a crack.*

For a certain plane of fracture, there are three possible types of relative displacements which can be referred to as modes of loading, modes of deformation, modes of cracking or modes of fracture. They are presented in Figure 3.2 and are denoted mode I, mode II and mode III. Mode I represent fracture due to pure tensile stress perpendicular to the plane of fracture, while mode II and III represents fracture due to in-plane shear stresses and transverse shear stress respectively. The general case consists of a mixture of the three modes but for most applications, the most common cases are modes I and II. Hence, the term *mixed mode* is often used to refer to a mixture of mode I and mode II only. [3] [11] [28] [29]

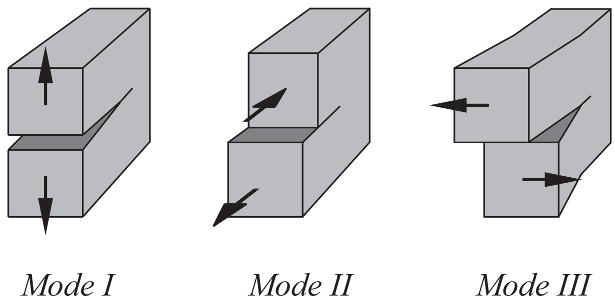

Figure 3.2: *Loading modes I, II and III.*

Energy release rate

One approach when analysing crack propagation is to consider the energy balance and how a virtual extension of the crack will effect the energy of the system. The energy release rate (sometimes also called the crack driving force) is defined according to Equation (3.7) as the decrease in potential energy U of the system at an infinitely small increase of the crack area A.

$$G = -\frac{\partial U}{\partial A} \tag{3.7}$$

The potential energy U of the system consists of elastic strain energy and the potential energy of the loads acting on the structure. The value of the energy release rate G is dependent on the geometry of the structure, the geometry of the crack, boundary conditions and applied loads. The dimension of G is energy/length^2 and the value can for some applications be determined analytically but is generally determined with numerical methods such as the finite element method. In order to determine whether a crack will propagate or not, the energy release rate is compared to the critical energy release rate G_c (sometimes also called the crack resistance) which is a material property. The general crack propagation criterion can thus be expressed as stated in Equation (3.8) which says that a crack is just about to propagate when the crack driving force equals the crack resistance or in other terms when the energy release rate equals its critical value.

$$G = G_c \tag{3.8}$$

As mentioned earlier, there are three possible modes of cracking and the critical energy release rate may have different values for the different modes. It is also possible to separate the energy release rate G into the three modes and obtaining G_I, G_{II} and G_{III}. The total energy release rate G_{tot} is then the sum of the contributions from G_I, G_{II} and G_{III}.

There are three possible scenarios when the crack is just about to propagate; stable, semistable and unstable crack growth. Unstable crack growth corresponds to the common case of increasing G with increasing crack area and hence an unstable crack growth. It is however also possible that G decreases with increasing crack area and if the value of G falls below the critical energy release rate G_c, the crack propagation will stop and the crack growth is termed stable. Semistable crack growth corresponds to the case when G is constant with increasing crack area. [3]

Stress intensity factor

Another approach for analysis of crack propagation is to consider the distribution of stresses in the vicinity of the tip of the crack by consideration of the stress intensity factors K_I, K_{II} and K_{III}. The definitions of these stress intensity factors are for the three modes of fracture given in Equations (3.9), (3.10) and (3.11) where stresses and coordinate system are defined in Figure 3.3. [31]

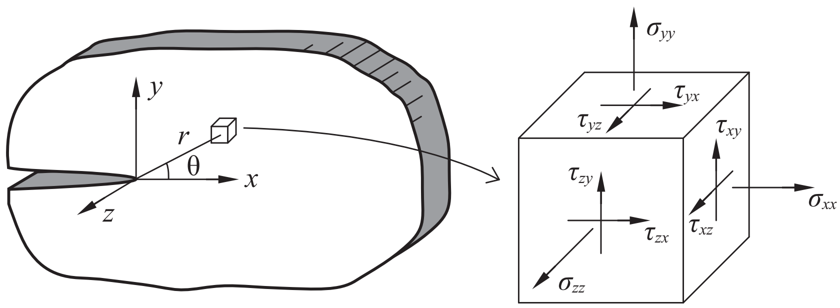

Figure 3.3: *Stresses used in definition of stress intensity factors.*

$$K_I = \lim_{r\to 0} \sigma_{yy}(r)\sqrt{2\pi r} \qquad \text{for } \theta = 0 \tag{3.9}$$

$$K_{II} = \lim_{r\to 0} \tau_{xy}(r)\sqrt{2\pi r} \qquad \text{for } \theta = 0 \tag{3.10}$$

$$K_{III} = \lim_{r\to 0} \tau_{yz}(r)\sqrt{2\pi r} \qquad \text{for } \theta = 0 \tag{3.11}$$

The values of the stress intensity factors are governed by the geometry of the structure, the geometry of the crack, boundary conditions and the applied load. The dimension of K is stress·length$^{1/2}$ or force·length$^{3/2}$. A crack will propagate when the stress intensity exceeds the critical stress intensity K_c (also known as the fracture toughness) according to Equation (3.12). Due to the linear elastic assumption, stresses and thereby also the stress intensity factors are proportional to the applied load.

$$K = K_c \tag{3.12}$$

For the case of mixed mode loading (Mode I and II), the crack propagation criterion according to Equation (3.13) purposed by Wu [30] has been verified by experimental tests and is frequently used with values $m = 1$ and $n = 2$.

$$\left(\frac{K_I}{K_{Ic}}\right)^m + \left(\frac{K_{II}}{K_{IIc}}\right)^n = 1 \tag{3.13}$$

Relation between G and K

The relationship between G_i and K_i for mode I and II for an orthotropic material considering a plane state of stress and a fracture plane which is oriented parallel to the direction of grain are as stated in the following equations. [3]

$$K_I = \sqrt{E_I G_I} \tag{3.14}$$

$$K_{II} = \sqrt{E_{II} G_{II}} \tag{3.15}$$

where

$$E_I = \sqrt{\frac{2E_x E_y}{\sqrt{\frac{E_x}{E_y}} + \frac{E_x}{2G_{xy}} - \nu_{yx}\frac{E_x}{E_y}}} \tag{3.16}$$

$$E_{II} = \sqrt{\frac{2E_x^2}{\sqrt{\frac{E_x}{E_y}} + \frac{E_x}{2G_{xy}} - \nu_{yx}\frac{E_x}{E_y}}} \tag{3.17}$$

In the above stated equations, E_x is Young's modulus parallel to grain, E_y is Young's modulus perpendicular to grain, G_{xy} is the shear modulus and ν_{yx} is Poisson's ratio.

J-integral method

The J-integral method, also known as Rice's integral method, is another commonly used method for crack propagation analysis. Considering a crack in a two-dimensional body as shown in Figure 3.4, the J-integral is calculated by integration of elastic strain energy density and stresses along a path Γ according to

$$J = \int_\Gamma \left(W dy - \sigma_{ij} n_j \frac{\partial u_i}{\partial x} ds\right) \tag{3.18}$$

where W is the elastic strain energy density, σ_{ij} are stresses, n_j the normal vector along the path of integration, u_i the displacement vector and s is the length of the path. The value of J is equal to the value of G and is also independent on the chosen path of integration as long as it starts and ends at opposite sides of the crack surface and encloses the tip of the crack. In the same manner as the energy release rate approach and the stress intensity factor approach, the value of J can for crack propagation analysis be compared to a critical value J_c. [3] [10]

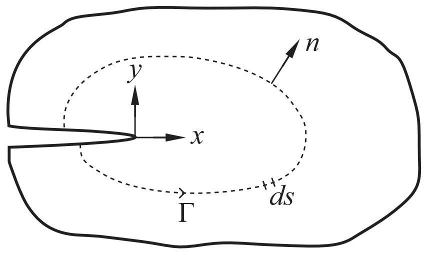

Figure 3.4: *Notations used in J-integral method.*

Other methods

There are also several other methods used in LEFM, for example the Crack closure integral method and Park's method. These methods are however not described here.

3.3 Generalized linear elastic fracture mechanics

The theory concerning linear elastic fracture mechanics presented in the previous section suffers from some obvious limitations: The theory is based on the assumption of an existing crack or a sharp notch giving rise to a square root stress singularity. Conventional stress analysis is on the other hand not applicable in the presence of a stress singularity. The LEFM-theory can be modified (generalized) in order to overcome this limitation and make it valid for more general cases. Two separate methods are presented here, the mean stress method and the initial crack method. These methods can be regarded as a combination of a conventional stress analysis and LEFM and have many features in common. Both methods yield the same results for a large body as LEFM if a large crack is present. For a large body in homogenous stress, they both yield the same results as a conventional analysis with a stress-based failure criterion. [6]

Mean stress method

The idea of the mean stress method is to consider the mean stresses acting on a possible fracture area and using them in a conventional stress-based failure criterion. The method can be used both for the case of a present stress singularity and the case of no stress singularity. For timber applications, the fracture plane is here assumed to coincide with the direction of grain due to the strength in tension perpendicular to grain being very low. For a mixed mode loading case, Norris' failure criterion according to Equation (3.19) can be used where $\overline{\sigma}_{90}$ and $\overline{\tau}$ are mean stresses.

$$\left(\frac{\overline{\sigma}_{90}}{f_t}\right)^2 + \left(\frac{\overline{\tau}}{f_v}\right)^2 = 1 \tag{3.19}$$

The size of the mean stress area is determined under the condition that the strength prediction will be the same as for Wu's crack propagation criterion according to Equation (3.13) and is hence governed by the stiffness, fracture energy and strength of the material. If only two dimensions are considered, the stress fields can be expressed according to the following expressions using the definitions of the stress intensity factors K_I and K_{II} according to Equations (3.9) and Equation (3.10).

$$\sigma_{90}(x) = \frac{K_I}{\sqrt{2\pi x}} + \ldots \tag{3.20}$$

$$\tau(x) = \frac{K_{II}}{\sqrt{2\pi x}} + \ldots \tag{3.21}$$

The first term in these series is dominating for small values of x. Denoting the length of which the mean stresses are calculated x_m and assuming only small values of x yields the following expressions for the mean stresses $\overline{\sigma}_{90}$ and $\overline{\tau}$.

$$\overline{\sigma}_{90} = \frac{\int_0^{x_m} \sigma_{90}(x)dx}{x_m} = \sqrt{\frac{2{K_I}^2}{\pi x_m}} \tag{3.22}$$

$$\overline{\tau} = \frac{\int_0^{x_m} \tau(x)dx}{x_m} = \sqrt{\frac{2K_{II}^2}{\pi x_m}} \tag{3.23}$$

Inserting $\overline{\sigma}_{90}$ and $\overline{\tau}$ in Equation (3.19), a general but rather complicated expression for x_m as a function of material properties (stiffness, fracture toughness, tensile- and shear strengths) and the mixed mode ratio $k = \overline{\tau}/\overline{\sigma} = K_{II}/K_I$ can be obtained. The expression can however be simplified for pure mode I or mode II loading where the E_I and E_{II} are stated in Equations (3.16) and (3.17) respectively.

$$x_m = x_m(E_{\parallel}, E_{\perp}, G, \nu_{\perp\parallel}, G_{ic}, f_t, f_v, k) \tag{3.24}$$

where

$$x_m = \frac{2}{\pi}\frac{E_I G_{Ic}}{f_t^2} \qquad \text{for pure mode I, } k = 0 \tag{3.25}$$

$$x_m = \frac{2}{\pi}\frac{E_{II} G_{IIc}}{f_v^2} \qquad \text{for pure mode II, } k \to \infty \tag{3.26}$$

Determination of the length x_m is an iterative process. A first guess of the length is needed and from this initial value the mean values $\overline{\sigma}_{90}$ and $\overline{\tau}$ are calculated which then results in a new mixed mode ratio from which the new length x_m is determined. [3] [6]

Initial crack method

The initial crack method is, as the name suggests, a way to overcome the prerequisite of a existing crack in LEFM. The procedure is such that a fictitious crack of length a_0 is added to the body where one would expect a crack to open up. The method can also be used for the case of an existing crack, then this crack is given a additional fictitious length a_0. The length a_0 is derived under the condition that the strength prediction for a large body without any stress singularity will be the same if using the initial crack method as if using the corresponding conventional stress criterion. Using this condition, derivation of a_0 is carried out in a similar manner as the derivation of x_m in the mean stress method which results in the following.

$$a_0 = \frac{x_m}{2} \quad \Longrightarrow \tag{3.27}$$

$$a_0 = \frac{E_I G_{Ic}}{\pi f_t^2} \quad \text{for pure mode I, } k = 0 \tag{3.28}$$

$$a_0 = \frac{E_{II} G_{IIc}}{\pi f_v^2} \quad \text{for pure mode II, } k \to \infty \tag{3.29}$$

The strength is calculated by a linear elastic fracture mechanics crack propagation criterion, for example by Wu's criterion according to Equation (3.13). [3]

3.4 Nonlinear fracture mechanics – NLFM

The term nonlinear fracture mechanics is ambiguous. In general, it refers to either analysis where a nonlinear stress-strain relationship of the material is considered or analysis where nonlinear fracture softening deformations in the fracture process region are taken into account. [6]

Fictitious crack model

The fictitious crack model was developed by Hillerborg et al at Lund University in the 1970's and takes the strain softening of the material into account. The theory is founded on the use of a conventional stress-strain relationship for stresses up to maximum stress and a stress-deformation relationship for the strain softening of the material. The deformation that determine the stress is the local additional deformation due to the gradual fracture of the material. A fracture zone is modeled as a fictitious crack which however can transfer stresses. The width w of the fictitious crack governs the stress distribution in the fracture zone while stresses outside of the fracture zone is determined from the general stress-strain relationship. The stress-deformation relationship can be approximated by piecewise linear polynomials. The finite element method is a suitable tool for FCM-analyses and can be performed on a body without initial cracks. The first step is to find the node that first reaches the maximum stress and hence is the place where the fracture zone develops. This node is separated into two nodes on opposite sides of the crack with a width w between them. The stress distribution in the fracture zone is then governed by the stress-deformation relationship. The next step is to increase the load to the point where maximum stress is reached in the next node along the path of the fracture zone and separating the next two nodes. The use of FCM is rather complex for timber applications since a propagating crack generally follows the direction of grain. This means that the direction of the crack is known but also that both shear stresses and normal stresses in the fracture zone needs to be taken into account. [11]

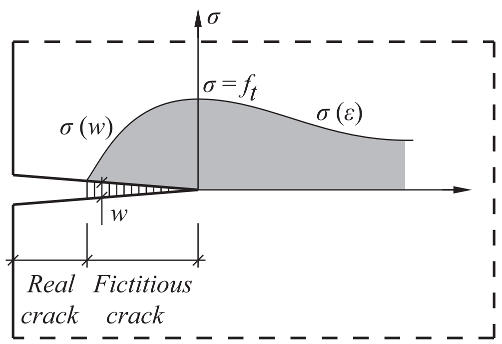

Figure 3.5: *Illustration of stresses in FCM [11].*

Quasi-nonlinear fracture mechanics

The term quasi-nonlinear fracture mechanics refers to analysis where a simplified stress-deformation relationship is derived from strength and fracture energy of the material is used. The shape of the true stress-deformation curve is assumed to have no influence and a linear relationship is instead used, which is derived in such way that the true strength is used and the slope is adjusted so that the area beneath the curve equals the fracture energy G_f. An illustration of a true and a simplified stress-deformation relationship is shown in Figure 3.6. [7]

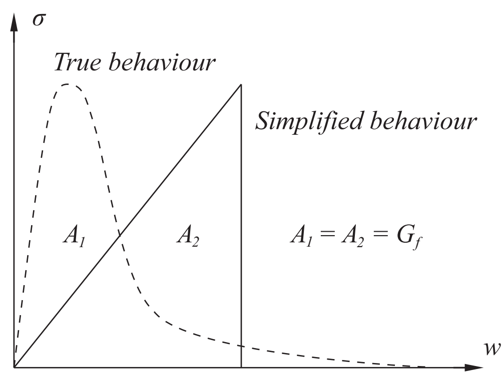

Figure 3.6: *Illustration of true and simplified stress-deformation relationship [7].*

3.5 Weibull weakest link theory

The Weibull weakest link theory enables a probabilistic based approach to strength analysis. This means that the probability of failure at a certain state of stresses for a certain volume of a material can be determined with knowledge of the strength and the scatter of the strength of the material. The strength perpendicular to grain is for wood strongly dependent on the size of the stress volume, the larger the volume the more likely it is that severe defects are present in the volume and thereby reducing the strength. This makes the theory very useful for timber applications considering the heterogeneity of the material due to annual rings, knots and other defects. The material is assumed to be ideally brittle and since fracture due to normal stresses perpendicular to grain or shear stresses parallel to grain are the most brittle fractures (although not ideally brittle) the theory applies well to these types of failure.

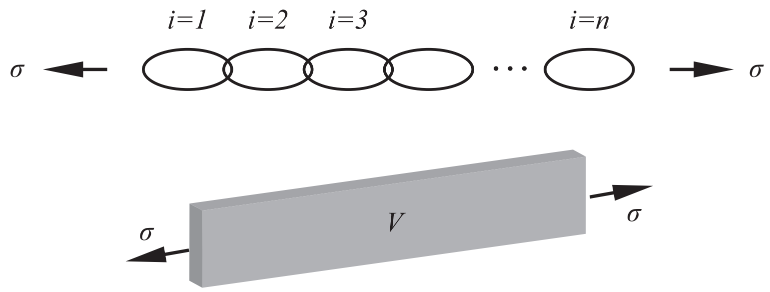

Figure 3.7: *Chain consisting of n discrete links (top) and volume V consisting of V/dV unit volumes dV (bottom).*

Consider a chain according to Figure 3.7 with n number of links loaded with a tensile stress σ. The nature of the structure is such that the chain will break as soon as one of the links break. The probability of failure of a link can be expressed according to Equation (3.30) where $f(\sigma)$ is a function of stress. The same equation can be used to describe the probability of failure in a unit volume dV of the volume V also shown in Figure 3.7.

$$S \;=\; 1 - e^{-f(\sigma)} \tag{3.30}$$

The probability of failure for a volume V exposed to a homogeneous or heterogeneous stress σ can be described by Equation (3.31). There are two purposed models for the function $f(\sigma)$, the 2-parameter model and the 3-parameter model according to Equations (3.32) and (3.33) respectively. The 2-parameter is the most used of the two models.

$$S = 1 - e^{-\int_V f(\sigma)dV} \tag{3.31}$$

$$f(\sigma) = \left(\frac{\sigma}{\sigma_0}\right)^m \qquad \text{2-parameter model} \tag{3.32}$$

$$f(\sigma) = \left(\frac{\sigma - \sigma_u}{\sigma_0}\right)^m \qquad \text{3-parameter model} \tag{3.33}$$

In the above stated equations, σ_0, σ_u and m are material parameters where the latter describes the scatter of the strength of the material. In order to be able to compare the probability of failure between different structures, a value called the effective Weibull stress, equivalent Weibull stress or Weibull stress is defined according to Equation (3.34).

$$\sigma_{wei} = \left(\frac{1}{V}\int_V \sigma^m(x, y, z)dV\right)^{1/m} \tag{3.34}$$

The effective Weibull stress is a fictive homogeneous stress that yields the same probability of failure as the the actual heterogenous state of stress. The influence of a heterogeneous stress distribution on the strength is described by the factor k_{dis} which is the ratio between the maximum value of the heterogeneous stress distribution and the Weibull stress.

$$k_{dis} = \frac{\sigma_{max}}{\sigma_{wei}} \tag{3.35}$$

The fictive strength f of a material with the volume V can be determined according to Equation (3.36) where f_{ref} is the strength of the material with the volume V_{ref}.

$$f = f_{ref}\, k_{dis} \left(\frac{V_{ref}}{V}\right)^{1/m} \tag{3.36}$$

[12] [13] [29]

3.6 Probabilistic fracture mechanics – PFM

In probabilistic fracture mechanics (PFM), both the heterogeneity of the material and the fracture ductility is considered. The heterogeneity of the material due to cracks, knots and other discontinuities can be treated by using for example Weibull theory or some other statistical method while the fracture ductility can be taken into account by the use of linear elastic-, generalized linear elastic- or nonlinear fracture mechanics. [29]

Chapter 4

Calculation approaches for beam with hole

This chapter presents brief summaries of some of the previously used calculation methods for strength analysis of glulam beams with holes.

4.1 Kolb and Frech, 1977

Kolb and Frech [20] determined the maximum normal stress due to bending and the maximum shear stress in the beam by Bernoulli-Euler beam theory. If the parts of the beam to the left and to the right of the hole are assumed to be stiff and the hole is placed centrically with respect to the height of the beam, the shear force is divided evenly between the upper and the lower part. They further tried to find a method where the tension force perpendicular to grain at the hole is taken into consideration. This was done by comparison to the case of an end-notched beam. An empirical expression based on a reduction of the shear force capacity with a factor determined by the relationship of the total height of the beam and the height of the upper or lower part of the beam at the hole was here used. This procedure resulted in an heavy underestimation of the capacity of the beams compared to the test results for all beams within the study.

4.2 Penttala, 1980

Penttala [21] used the plate theory with complex functions proposed by Kolosov and Muskhelishvili to analytically determine the state of stresses. For the beams with circular holes, both isotropic and anisotropic material models were used while for beams with rectangular holes, only isotropic material models were used. The stress at the edge of the hole was compared to the material strength in tension which was determined by Hankinson's formula as a function of grain angle.

4.3 Johannesson, 1983

Johannesson [14] used three separate methods when analysing the strength of the tested beams.

”Shear-stress” method

This is an empirically based method which formally reads as a comparison between shear stress and a fictive shear strength determined from experimental tests. The fictive shear strength was determined by calculation of the shear stresses at cracking with the assumption of a parabolic stress distribution. A relationship between geometric parameter D/H and the fictive shear strength was established, where D is the diagonal of a rectangular hole or the diameter in the case of a circular hole while H is the height of the beam. Among other simplifications, the effects of bending moment are not taken into account using this method which hence must be considered merely as a tool for rough estimations. One of the methods suggested for design of glulam beams with holes in the Swedish code of practise, *Limträhandbok*, presented in Chapter 5 is based on this method.

”Navier-beam” method

The ”Navier-beam” method was developed to enable hand calculations that are more reliable compared to the ”Shear-stress” method. Cross sectional forces are determined from equilibrium conditions and a linear stress distribution in a stress plane at the corners where the beam is exposed to tension perpendicular to grain are assumed according to Navier’s theory. The maximum hoop stress in this plane is compared to a corresponding strength parameter determined from material tests.

”Exact-stress” method

Three separate methods were used within the so called ”Exact-stress” method when determining the perpendicular to grain stresses for holes with rounded corners; closed form analytical solution, the finite element method and the boundary element method. Some assumptions were made in order to simplify the analyses. A linear elastic material model was used for all analyses and a plane state of stress was assumed based on the fact that the beam width was small in comparison to the height and the length of the beam. Thus, the influence of the cylindrical shape of annual rings was ignored and a two-dimensional orthotropic material model was instead used. Further, the deformations were assumed to be small, the beam is assumed to be in equilibrium and the failure criterion according to Equation (3.2) was used. Johannesson found that this criterion could be simplified for the applications in mind by ignoring all terms but the second one. The problems is then decreased to finding the stress σ_2 and the strength parameter f_2 perpendicular to grain.

4.4 Pizio, 1991

Pizio [23] used a linear elastic fracture mechanics approach and determined stress intensity factors numerically by using finite elements. Three different methods were used; Park's method, the Rice Integral method and the Crack Closure Integral method. Initial cracks were modeled at the corners exposed to tensile stresses perpendicular to grain which then grew in the length direction of the beam (parallel to grain). The beams were modeled as a homogeneous and orthotropic material with a plane state of stress. It was further assumed that the fractures were of mixed modes, mode I and mode II. Experimental material testing was carried out in order to determine fracture mechanics material properties.

4.5 Hallström, 1995

Hallström [8] [9] investigated the stress distribution and stress intensity factors for unreiforced and reinforced glulam beams with holes. The stress distribution at the vicinity of the corners of the holes was analytically determined in two dimensions using an orthotropic material model. Finite element analyses where also carried out in three dimensions using transversely isotropic material model. Linear elastic fracture mechanics analyses were also performed with initial cracks of various lengths at critical locations which for rectangular holes with sharp corners are the corners. For rectangular holes with rounded corners and circular holes respectively, calculation were first made in order determine where cracks were to expect. These initial cracks were modeled in the complete beam width and parallel to grain direction.

4.6 Riipola, 1995

Riipola [24] [25] analysed timber beams and glulam beams with holes with a linear elastic fracture mechanics approach and considering the energy balance. Analytical expressions for the strain energy release rates for mode I and mode II type of fracture were derived separately and the stress intensity factors were then determined from these expressions. By comparison of the stress intensity factors and experimentally determined critical stress intensity factors according to Wu's fracture criterion stated in Equation (3.13), the load bearing capacities were evaluated. The method is valid for holes which are placed in a shear force dominated area. For holes placed close to support, an extra correction factor was used.

4.7 Aicher, Schmidt and Brunhold, 1995

Aicher, Schmidt and Brunhold [1] used linear elastic fracture mechanics and the finite element method to calculate stress intensity factors K_i and energy release rates G_i. Two separate methods were used. The stress intensity factors K_i were determined by substitution of the displacements at the crack tip into closed form expressions. The energy release rates G_i were determined using a method based on a virtual crack closure integral. A two dimensional model was used for all calculations and mixed mode I and mode II fracture was considered. Wu's interaction criterion according to Equation (3.13) was used when analysing the load bearing capacity.

4.8 Petersson, 1995

Petersson [22] analysed wooden beams where fracture due to tension perpendicular to grain are common. He used linear elastic fracture mechanics and an energy based approach. Finite element calculations were performed in two dimensions under the assumption of a plane state of stress and with linear elastic, orthotropic material properties. Dynamic and nonlinear geometric effects were not taken into consideration. In order to determine the mixed mode crack state and the appropriate value of the material parameter G_c, nodal forces in the elements close to the crack tip were studied.

4.9 Gustafsson, Peterson and Stefansson, 1996

Gustafsson, Peterson and Stefansson [5] used the initial crack method and the mean stress method, both generalized linear elastic fracture mechanics methods, to predict load bearing capacity for timber beams. Another method was also used, which basically is an engineering estimation of the load bearing capacity based on the relationship between crack propagation load and crack length. Plane stress and linear elastic orthotropic material properties were assumed for all analyses. Gustafsson also presents these generalized linear elastic fracture mechanics methods in [3] where also examples of application to beams with a hole are indicated.

4.10 Scheer and Haase, 2000

Scheer and Haase [26] used analytical formulations according to Lekhnitskii and Savin to determine stress concentrations near elliptical holes in glulam beams. The finite element method was also used in order to verify the analytical solutions. For the analytical calculations, the beam was modeled as a plate with a plane state of stress and orthotropic material properties.

Scheer and Haase [27] also used a fracture mechanics approach and determined stress intensity factors at fictitious cracks with the finite element method and the Rice integral. The beam was modeled in two dimensions as an orthotropic material and the two existing symmetry planes were used in order to decrease the size and thereby the calculation cost. The fictitious cracks were modeled parallel to grain with independently varying length (1-10 mm) and location along the hole periphery. Varying load cases were investigated and the stress intensity factors for mode I and mode II type of failure were calculated for all different lengths and locations of the fictitious crack. Wu's failure criterion according to Equation (3.13) was used.

4.11 Stefansson, 2001

Stefansson [28] performed strength analyses on timber beams with circular and quadratic holes using linear elastic fracture mechanics and nonlinear fracture mechanics in finite element analyses. In the LEFM analyses, a crack was modeled in a critical region and strength was analysed for various lengths of this crack using the energy release rate approach. A plane state of stress was assumed and a linear elastic and orthotropic material model was used. The NLFM analyses are based on the fictitious crack model and applied by means of interface elements with a piecewise linear stress-deformation relationship on a prescribed crack path.

4.12 Höfflin, 2005

Höfflin [12] performed several different numerical analyses in order to examine the state of stresses in the hole vicinity of the glulam beams. Both 2D and 3D finite element analyses were carried out.

Conventional stress analysis - 2D FEM

The analyses were in two dimensions performed assuming plane state of stress and an orthotropic material model. The distribution of the stress components σ_x, σ_y and τ_{xy} along the hole perimeter was first investigated and the value and location of the maximum tensile stress perpendicular to grain were then determined. This procedure results in knowledge of where along the hole perimeter the largest stresses perpendicular to grain appear and thus also where to expect a crack to open up.

Conventional stress analysis - 3D FEM

Depending on the orientation of the annual rings in the lamellae, the stress perpendicular to grain can vary significantly across the beam width. This variation is disregarded when assuming plane stress conditions. Three dimensional models of the beams make it possible to more accurately model the material properties of the glulam. This can be done by modeling each lamella as a cylindrically anisotropic material. Modeling a complete beam geometry this way is rather demanding and results in large computational cost. Höfflin instead used a combination of two- and three dimensional models using the so called *Submodel technique*. The complete beam was modeled in two dimensions and only a small part of the beam (1/2 of beam height) near the hole was modeled in three dimensions. The 2D model of the complete geometry was used to determine the appropriate boundary conditions to use for the 3D model. The 3D model was also simplified by assigning cylindrical anisotropic properties only to the lamellae crossed by the hole and assigning orthotropic properties to the other lamellae. This procedure is more complex compared to the 2D analysis but should also give more realistic results since the orientation of annual rings can be taken into account. There is however a long list of parameters to adjust.

Weibull weakest link theory

Höfflin also used Weibull theory and determined the ratio between the maximum stress at an uneven stress distribution and the equivalent Weibull stress corresponding to the same probability of failure. This ratio is a form factor which represents the level of heterogeneity in the material and the stress distribution. The calculations are to a great extent dependent on the stressed area chosen for integration. Several different shear force to bending moment ratios were also investigated. A method for design of glulam beams with circular holes based on Weibull weakest link theory is proposed.

Chapter 5

Design codes

Determination of the load bearing capacity of glulam beams with holes is by no means a trivial task which is also reflected the guidelines from different contemporary and previous design codes. The design rules vary significantly between different codes, where some design rules are empirically based and others are more rationally based. This chapter presents the rules for design according to some European codes and also a comparison of experimental test results with strengths according to codes.

5.1 Swedish code of practise – *Limträhandbok*

The Swedish *Limträhandbok* (Glulam handbook) [41] is not an official Swedish norm but rather a tool for recommendations concerning design of glued laminated timber. Two possible methods are presented for design of glulam beams with holes, one is empirically based and the other is based on estimation by means of comparison with fracture mechanics analysis of end-notched beams.

For both methods, there are some basic recommendations concerning size and placement of the hole. First and foremost, all holes in glulam beams should as far as possible be avoided. If a hole cannot be avoided, it should be placed with its center in the neutral axis of the beam. A discrepancy of no more than 10 % of the beam height H is tolerable. Furthermore, the hole height b (or ϕ) may not exceed $H/2$ and the hole length a may not exceed $3b$. If two holes are placed in the same beam, the distance between hole edges must be at least the same as the height H of the beam. The corners of rectangular holes must have a radius $r \geq 25$ mm. Measures should be taken in order to decrease the risk of cracks in the hole surface due to a varying moisture content in the beam.

Method 1 – Empirically based design

The capacity with respect to bending moment and shear force should be controlled separately for the net cross section at the hole, see Figure 5.1. The shear force criterion is formulated to compare the shear stress τ to the reduced shear strength $f_{v,red}$ of the cross section through the hole according to Equation (5.1). Both the upper and the lower part need to be controlled, index i represents the upper (u) or lower (l) part of the beam at the hole. The shear force may be assumed to be divided between the upper and the lower part according to the relation of stiffness between the two parts but no further instructions are given on how to divide the force between the two parts. The shear strength is reduced depending on the size and shape of the hole by the factor k_{hole} while a beam width dependent volume effect is taken into account by the factor k_{vol}. Beams where the width T is less than 90 mm were not included in the study on which the design method is based.

For rectangular holes, the additional bending moment caused by the shear force should also be considered. If there is less then four lamellae in the upper or the lower part, the design strength with respect to bending should be decrease 25 %. No further instructions are given on how the bending capacity should be checked.

$$\tau = \frac{1.5V_i}{Th_i} \leq f_{v,red} \qquad \text{where index } i = u \text{ or } l \tag{5.1}$$

$$f_{v,red} = k_{vol} k_{hole} f_v \tag{5.2}$$

$$k_{vol} = \left(\frac{90}{T}\right)^{0.2} \qquad \text{for } 90 \leq T \leq 215 \text{ mm} \tag{5.3}$$

$$k_{hole} = \begin{cases} 1 - 555(D/H)^3 & \text{for } D/H \leq 0.1 \\ \dfrac{1.62}{(1.8 + D/H)^2} & \text{for } D/H > 0.1 \end{cases} \tag{5.4}$$

$$\text{where } D = \begin{cases} \sqrt{b^2 + a^2} & \text{for rectangular hole} \\ \phi & \text{for circular hole} \end{cases}$$

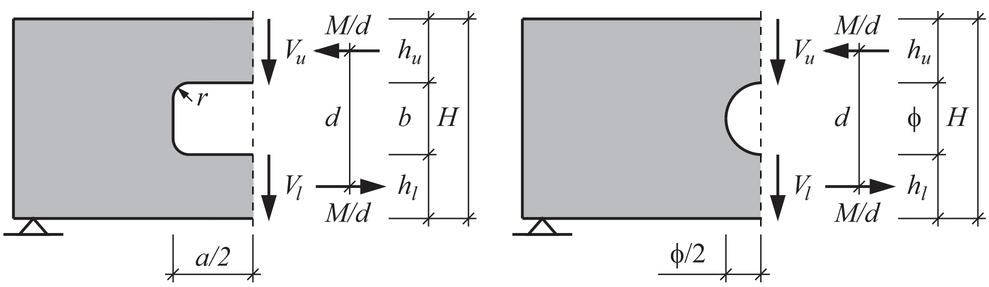

Figure 5.1: *Notations for design according Method 1, Swedish Limträhandbok.*

Method 2 – "End-notched beam" analogy

Limträhandbok suggests an alternative design method for holes placed in a shear force dominated region. The stress distribution in the vicinity of a hole is considered to be rather alike that at an end-notched beam and the design recommendations are hence based on the method for design of an end-notched beam.

As for method 1, the design criterion is formulated to compare the shear stress τ to the reduced shear strength $f_{v,red}$ according to Equation (5.5). Since the hole is assumed to be placed in a shear force dominated region, the effects of any bending moment are disregarded. For a hole placed centrically in the beam, the shear forces V_u and V_l are equal to $V/2$.

The shear strength is reduced depending on whether the considered part is exposed to tensile or compressive stresses perpendicular to grain. The factor $k_{v,i}$ is equal to 1 for the lower parts in Figure 5.2 but ≤ 1 for the upper parts since they are exposed to tensile stresses perpendicular to grain. What is considered to be the upper or lower part is hence dependent on the direction of the shear force V.

$$\tau = \frac{1.5V_i}{Th_i} \leq f_{v,red} \qquad \text{where index } i = u \text{ or } l \tag{5.5}$$

$$f_{v,red} = k_{v,i} f_v \tag{5.6}$$

$$k_{v,l} = 1.0 \tag{5.7}$$

$$k_{v,u} = \min \begin{cases} 1.0 \\ \dfrac{6.5\left(1 + \dfrac{1.1 j^{1.5}}{\sqrt{h}}\right)}{\sqrt{h}\left(\sqrt{\alpha - \alpha^2} + 0.8\dfrac{e}{h}\sqrt{\dfrac{1}{\alpha} - \alpha^2}\right)} \end{cases} \tag{5.8}$$

where for holes placed centrically in the beam height

$h = H/2 \qquad$ [mm]

$\alpha = h_u/h$

$$j = \begin{cases} 0 & \text{for rectangular hole} \\ 1.0 & \text{for circular hole} \end{cases}$$

$$e = \begin{cases} a/2 & \text{for rectangular hole} \\ 0 & \text{for circular hole} \end{cases}$$

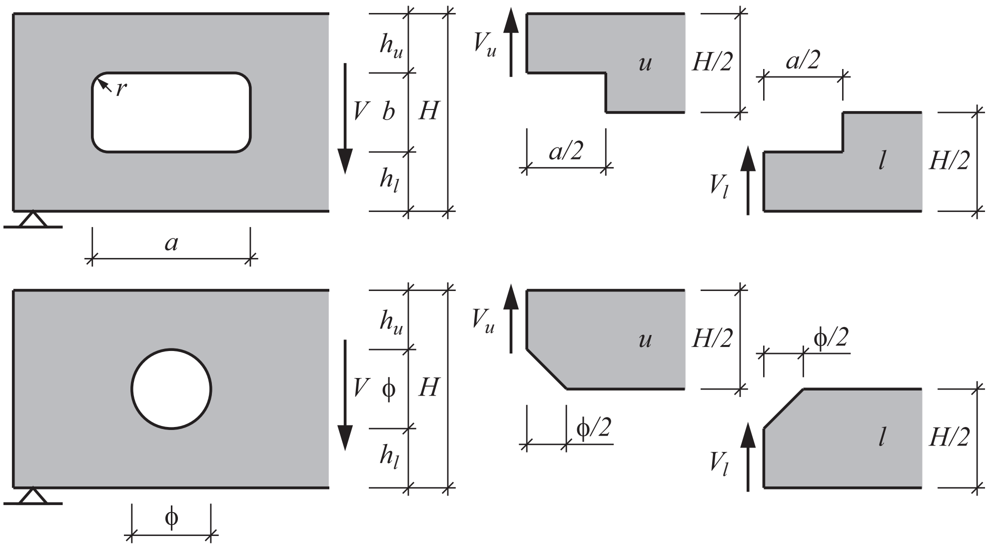

Figure 5.2: *Notations for design according Method 2, Swedish Limträhandbok.*

5.2 German code – DIN 1052

DIN 1052:2004-08

The design rules concerning the capacity of glulam beams with holes are treated rather differently in the German code DIN 1052 [33] compared to the two methods in *Limträhandbok*. The German code states that special attention must be given when designing a glulam beam with a hole. A hole is defined as an opening with $\sqrt{a^2+b^2} - r(\sqrt{2}-1)$ or ϕ greater than 50 mm for rectangular or circular openings respectively. Other openings should however be designed as a reduced cross section (Ger. *Querschnittsschwächung*).

The general requirements concerning hole geometry and placement are similar to the requirements in *Limträhandbok*. The hole must be placed with a distance from hole edge to end of beam equal to or greater than the beam height H. The distance from hole edge to center of support must be greater or equal to $H/2$. If two holes are placed in the same beam, the distance between them must be at least the same as the height H but also never shorter than 300 mm. The length of the hole a should be less or equal to the height H of the beam and the height of the hole b or ϕ may not exceed $0.4H$. The height of remaining parts of the beam (h_u and h_l) must be at least $H/4$. The corners of rectangular holes must be rounded with a corner radius $r \geq 15$ mm.

Holes that fulfill the above given requirements may be used in the service class (Ger. *Nutzungsklasse*) 1 and 2 but the hole must however be reinforced for use in service class 3. The capacity of the beam at the hole is determined by Equation (5.9) where $F_{t,90,d}$ is the design tension force perpendicular to grain and $l_{t,90}$ the assumed length of the triangular shaped normal stresses perpendicular to grain. The design tension force is determined from contributions by the design shear force V_d and the design bending moment M_d. Both sections 1 and 2 according to Figure 5.3 should be controlled.

$$F_{t,90,d} \leq 0.5 l_{t,90} T f_{t,90,d} \tag{5.9}$$

$$l_{t,90} = \begin{cases} 0.5(b+H) & \text{for rectangular hole} \\ 0.353\phi + 0.5H & \text{for circular hole} \end{cases}$$

$$F_{t,90,d} = F_{t,V,d} + F_{t,M,d} \tag{5.10}$$

$$F_{t,V,d} = \frac{V_d x}{4H}\left(3 - \frac{x^2}{H^2}\right) \tag{5.11}$$

$V_d =$ Design value of shear force section 1 or 2

$$x = \begin{cases} b & \text{for rectangular hole} \\ 0.7\phi & \text{for circular hole} \end{cases}$$

$$F_{t,M,d} = 0.008 \frac{M_d}{h_r} \tag{5.12}$$

$M_d =$ Design value of bending moment at section 1 or 2

For rectangular holes

$$h_r = \min \begin{cases} h_u \\ h_l \end{cases}$$

For circular holes

$$h_r = \min \begin{cases} h_u + 0.15\phi \\ h_l + 0.15\phi \end{cases}$$

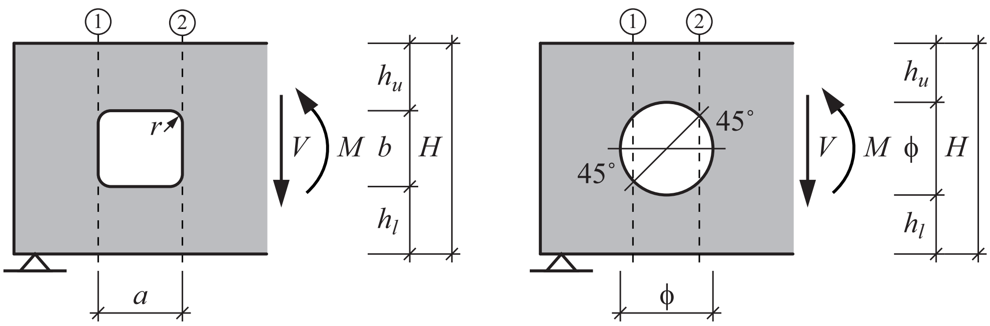

Figure 5.3: *Notations for rectangular and circular holes for design according to DIN 1052:2004-08.*

DIN 1052:1999

An older version of the German code, DIN 1052:1999 [34], differs somewhat from the contemporary version. The difference lies in the contribution from the shear force to the design tension force perpendicular to grain where the older version states a more complex expression. For beams with rectangular holes which are centrically placed with respect to the beam height, Equation (5.14) reduces to Equation (5.11) stated in contemporary version DIN 1052:2004. The parameter x is for circular holes different compared to the contemporary code.

$$F_{t,90,d} = F_{t,V,d} + F_{t,M,d} \tag{5.13}$$

$$F_{t,V,d} = V_d \left[3h_r^2 \left(\frac{1}{(H-x)^2} - \frac{1}{H^2} \right) - 2h_r^3 \left(\frac{1}{(H-x)^3} - \frac{1}{H^3} \right) \right] \tag{5.14}$$

$V_d =$ Design value of shear force at hole edge

$$x = \begin{cases} b & \text{for rectangular hole} \\ \phi & \text{for circular hole} \end{cases}$$

For rectangular holes

$$h_r = \min \begin{cases} h_u \\ h_l \end{cases}$$

For circular holes

$$h_r = \min \begin{cases} h_u + 0.15\phi \\ h_l + 0.15\phi \end{cases}$$

5.3 European code – *Eurocode 5*

EN 1995-1-1:2004

Design of glulam beams with holes are not explicitly stated in latest version of *Eurocode 5*, EN 1995-1-1:2004 (E) [38]. There is however a section on design of notched members and end-notched beams. The design procedures for these cases are identical to those stated in *Limträhandbok* concerning end-notched beams, see Section 5.1.

prEN 1995-1-1:Final Draft 2002-10-09

A previous version of *Eurocode 5*, prEN 1995-1-1:Final Draft 2002-10-09 [39], had a section on design of glulam beams with holes. The analogy with end-notched beams was used in the same manner as described in Method 2 from *Limträhandbok*. The design rules are identical although the shear force for the upper and lower parts are specified explicitly according to Equations (5.15) and (5.16).

$$V_u = V \frac{h_u}{h_u + h_l} \tag{5.15}$$

$$V_l = V\frac{h_l}{h_u + h_l} \tag{5.16}$$

The capacity with respect to axial loads and bending moment should be evaluated for the reduced cross section at the hole. Holes with $\sqrt{a^2+b^2} - r(\sqrt{2}-1)$ or ϕ less than 50 mm and less than $0.1H$ may be disregarded. The regulations concerning hole geometry and placement are identical to those stated for the German code DIN 1052.

5.4 Swiss code – SIA 265

The Swiss code for timber structures, SIA 265 [36], states that holes exposed to a large shear force (holes placed close to support) may be *approximately* designed in the same manner as an end-notched beam. The analogy is shown in Figure 5.4. The following design rules are stated for an end-notched beam where f_v is the allowed shear stress. It seems as if the length of a rectangular hole is in no way considered using this approach.

$$\tau = \frac{1.5V_d}{Th_{ef}} \leq f_{v,red} \tag{5.17}$$

$$f_{v,red} = k_{red} f_v$$

$$k_{red} = \begin{cases} \sqrt{\dfrac{h_{ef}}{h}\dfrac{\Delta h_0}{\Delta h_{ef}}} \leq 1 & \text{for tension perpendicular to grain} \\ 1 & \text{for compression perpendicular to grain} \end{cases}$$

$$\Delta h_0 = 45 \text{ mm}$$

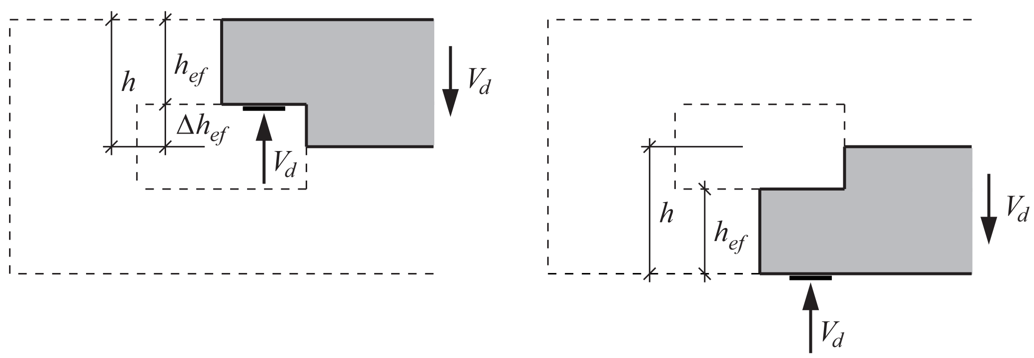

Figure 5.4: *Notations for design according to SIA, tension perpendicular to grain (left) and compression perpendicular to grain (right).*

5.5 Comparison between tests and design codes

The previous sections of this chapter reveals fundamental differences concerning design methods between the codes. In order to make some evaluation of the presented design codes, the characteristic shear force capacity V_k according to the different methods was calculated for all beams with a hole in a shear force dominated region. The characteristic shear strength $f_{v,k} = 4$ MPa was used for calculations according to method 1 and 2 according to *Limträhandbok* and calculations according to SIA 265 while characteristic tension perpendicular to grain strength $f_{t,90,k} = 0.5$ MPa was used for calculations according to German code DIN 1052. These results and the mean values of the experimental test results for all test series with holes placed in shear force dominated region are presented in Table 5.2 for beams with circular holes and in Table 5.3 for beams with rectangular holes.

Graphical comparison of the codes and comparison of the results of the experimental tests and the codes are presented in Figures 5.6-5.23. The characteristic capacity according to codes and the experimental test results are presented as the mean shear stress V/A_{net} where A_{net} is the net cross section area at the vertical section through the center of hole. The test results are in these figures represented by the crack load V_c for the individual tests. The hole design is described by the ratio D/H where $D = \phi$ for circular holes and $D = \sqrt{a^2 + b^2}$ for rectangular holes. In the figures, solid lines represent hole dimensions which are within the regulations stated in the code. Since all test series have holes which are centrically placed with respect to the beam height, all graphs describing capacities according to codes are also based on this assumption.

The same shear strength $f_{v,k}$ (4.0 MPa) are used for all calculations although the value differs between the strength classes found among the test series, see Table 2.3. The value of the perpendicular to grain tensile strength $f_{t,90}$ is the same for all glulam strength classes except Klasse B depending on the SIA 265 using allowable stress and not characteristic material strengths.

Since the capacities according to codes here are determined from the characteristic strengths, the ratio V_c/V_k should be somewhat greater than 1.0 for satisfactory design. Although, the terms *overestimation* and *underestimation* are here simply used to described whether the characteristic capacity according to code are higher or lower than the mean values or the individual values of the experimental test results.

Some specific observations from the presented tables and figures are worth pointing out:

- Many of the test series, especially test series with rectangular holes, have hole sizes and/or hole placements and/or corner radii which are not within the allowed boundaries stated in the different codes.

- Method 1 according to *Limträhandbok* underestimates the capacity for all test series except for two series with circular holes. Common for these exceptions are that large beams ($H = 900$ mm) are used in both series and the holes are subjected to comparatively large bending moment ($M/(VH) = 5.0$).

- Method 2 according to *Limträhandbok* overestimates the capacity for all test series with circular holes and for the majority of the test series with rectangular holes. For test series with circular holes, the ratio V_c/V_k varies within a narrow range compared to the Method 1 and to the other codes.

- DIN 1052:2004 overestimates the capacity for five of the test series with circular holes. Four out of these five are test series with large beams ($H = 900$ mm) and the fifth test series has a hole twice the maximum acceptable size stated in the code.

- Only two test series with rectangular holes have a hole size, placement and corner radius in accordance with the regulations in DIN 1052. The ratios V_c/V_k are for these test series 1.38 and 1.31 while the same ratio varies within the range $0.29 \leq V_c/V_k \leq 1.86$ for the other test series.

- In method 1 according to *Limträhandbok*, there is a beam width size effect taken into account but no beam height size effect.

- There is no size effect taken into account in DIN 1052.

- The Swiss code SIA 265 overestimates the capacity for most of the test series with circular holes and for all but two test series with rectangular holes. The shear force capacity according to SIA is independent of the hole side length a of a rectangular hole.

- All test series with rectangular holes and recorded crack loads V_c have a beam height $H \leq 585$ mm.

The regulations concerning hole size, corner radius and hole placement in relation to support, to other holes and to the neutral axis differ between the codes. The regulations in the older version of *Eurocode 5* (prEN 1995-1-1:Final Draft) are identical to the ones in the German code DIN 1052 (both the contemporary and the older version) but these differs somewhat from the regulations in *Limträhandbok*. A comparison is presented in Table 5.1 and the notations are found in Figure 5.5. There are no explicit rules concerning hole geometry or placement stated in the the Swiss code SIA 265.

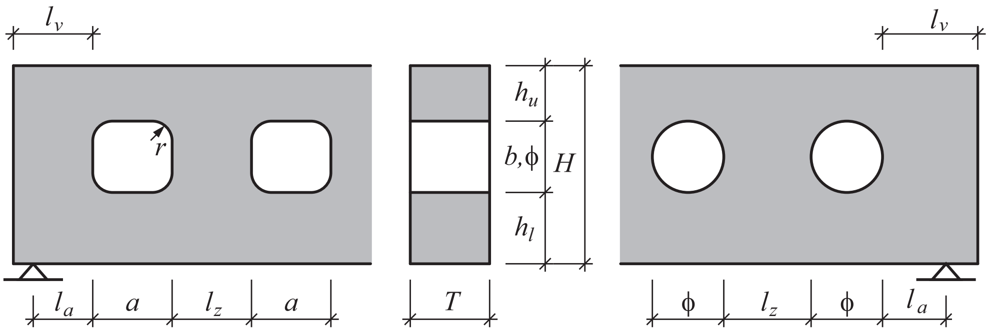

Figure 5.5: *Notations for regulations concerning hole geometry and placement.*

Table 5.1: *Regulations concerning hole geometry and placement.*

	Limträhandbok [41]	DIN 1052:2004 [33] DIN 1052:1999 [34] prEN 1995-1-1 [39]
l_a	-	$\geq 0.5H$
l_v	-	$\geq H$
l_z	$\geq H$	$\geq H$ and $\geq$ 300mm
h_u	$\geq 0.15H$	$\geq 0.25H$
h_l	$\geq 0.15H$	$\geq 0.25H$
a	$\leq 3b$	$\leq H$
b or ϕ	$\leq 0.5H$	$\leq 0.4H$
r	≥ 25 mm	≥ 15 mm

Table 5.2: *Experimental test results of beams with circular holes.*

Test series notation	Beam $H \times T$ [mm^2]	Hole design ϕ [mm]	$\frac{D}{H}$ [-]	$\frac{M}{VH}$ [-]	n	V_{c0} Mean [kN]	V_c Mean [kN]	V_f Mean [kN]
BEN-1	500 × 90	ϕ250	0.50	1.20	2			38.4
BEN-3	500 × 90	ϕ150	0.30	1.20	1			52.5
PENa-1	500 × 90	ϕ255	0.51	1.20	1			33.8
PENa-2	500 × 90	ϕ250	0.50	2.10	1			31.6
PENa-3	500 × 90	ϕ150	0.30	1.20	1			51.3
PENb-1	800 × 115	ϕ400	0.50	1.03	1	57.1		65.9
PENb-2	800 × 115	ϕ300	0.38	2.00	1			89.5
JOHa-1	500 × 90	ϕ250	0.50	1.30	2		29.6	36.5
JOHa-3	500 × 90	ϕ250	0.50	2.80	2		33.2	37.5
JOHa-5	500 × 90	ϕ250	0.50	0.60	2		33.8	41.7
JOHa-6	500 × 90	ϕ125	0.25	0.60	2		-	40.1
JOHd-1	495 × 88	ϕ125	0.25	2.53	4		51.9	
JOHd-2	495 × 88	ϕ396	0.80	2.53	4		16.1	
HALa-3	315 × 90	ϕ150	0.48	2.78	5		24.5	
HOFa-1	450 × 120	ϕ90	0.20	1.50	5	62.8	76.8	82.1
HOFa-2	450 × 120	ϕ135	0.30	1.50	6	38.8	65.5	67.9
HOFa-3	450 × 120	ϕ180	0.40	1.50	4	34.6	47.6	51.8
HOFb-1	900 × 120	ϕ180	0.20	1.50	5	69.2	106.4	128.1
HOFb-2	900 × 120	ϕ270	0.30	1.50	6	65.3	96.4	108.7
HOFb-3	900 × 120	ϕ360	0.40	1.50	6	48.0	69.2	87.5
HOFc-1	450 × 120	ϕ135	0.30	5.00	5	34.7	58.0	63.4
HOFd-1	900 × 120	ϕ270	0.30	5.00	5	43.1	55.1	84.2
AICa-1	450 × 120	ϕ180	0.40	5.00	6	42.4	48.8	53.7
AICb-1	900 × 120	ϕ180	0.20	5.00	4	66.4	106.4	111.6
AICb-2	900 × 120	ϕ360	0.40	5.00	5	46.7	61.6	79.9
AICc-1	450 × 120	ϕ180	0.40	5.00	3	15.4	37.9	44.8
AICd-1	900 × 120	ϕ360	0.40	5.00	3	33.5	49.6	66.6

Test series notation	Limträhandbok Method 1 V_k [kN]	V_c/V_k [-]	Limträhandbok Method 2 V_k [kN]	V_c/V_k [-]	DIN 1052 2004 V_k [kN]	V_c/V_k [-]	DIN 1052 1999 V_k [kN]	V_c/V_k [-]	SIA 265 V_k [kN]	V_c/V_k [-]
BEN-1	18.4		52.8		26.6 [1]		15.0 [1]		25.5	
BEN-3	30.9		80.6		37.5		24.5		54.4	
PENa-1	17.9 [1]		51.7 [1]		26.3 [1]		14.7 [1]		24.5	
PENa-2	18.4		52.8		24.7 [1]		14.4 [1]		25.5	
PENa-3	30.9		80.6		37.5		24.5		54.4	
PENb-1	35.8		84.1		55.3 [1]		31.0 [1]		41.1	
PENb-2	50.0		108.6		61.0		39.0		66.4	
JOHa-1	18.4	1.61	52.8	0.56	26.4 [1]	1.12	15.0 [1]	1.91	25.5	1.16
JOHa-3	18.4	1.81	52.8	0.63	23.4 [1]	1.42	14.0 [1]	2.38	25.5	1.30
JOHa-5	18.4	1.84	52.8	0.64	28.1 [1,2]	1.20	15.5 [1,2]	2.18	25.5	1.33
JOHa-6	34.7		90.0		46.2 [2]		30.3 [2]		66.1	
JOHd-1	34.1	1.52	86.8	0.60	35.3	1.47	24.8	2.09	63.7	0.81
JOHd-2	5.7 [1]	2.83	23.2 [1]	0.69	17.8 [1]	0.90	9.0 [1]	1.80	5.0	3.28
HALa-3	12.4	1.98	39.6	0.62	15.2 [1]	1.61	9.2 [1]	2.65	22.2	1.10
HOFa-1	44.0	1.74	115.2	0.67	57.7	1.33	40.5	1.90	103.0	0.75
HOFa-2	35.0	1.87	100.8	0.65	43.6	1.50	28.8	2.27	68.9	0.95
HOFa-3	27.3	1.74	82.0	0.58	35.9	1.33	22.2	2.15	47.3	1.01
HOFb-1	88.1	1.21	185.6	0.57	115.4	0.92	81.0	1.31	145.7	0.73
HOFb-2	69.9	1.38	141.8	0.68	87.2	1.11	57.5	1.68	97.4	0.99
HOFb-3	54.6	1.27	113.7	0.61	71.8	0.96	44.4	1.56	66.9	1.03
HOFc-1	35.0	1.66	100.8	0.58	31.6	1.83	23.0	2.52	68.9	0.84
HOFd-1	69.9	0.79	141.8	0.39	63.3	0.87	46.0	1.20	97.4	0.57
AICa-1	27.3	1.79	82.0	0.59	27.2	1.80	18.5	2.64	47.3	1.03
AICb-1	88.1	1.21	185.6	0.57	86.5	1.37	57.6	1.76	145.7	0.73
AICb-2	54.6	1.13	113.7	0.54	54.3	1.13	37.0	1.67	66.9	0.92
AICc-1	27.3	1.39	82.0	0.46	27.1	1.40	18.5	2.05	47.3	0.80
AICd-1	54.6	0.91	113.7	0.44	54.3	0.91	37.0	1.34	66.9	0.74

[1] = Size of hole not within regulations.
[2] = Placement of hole not within regulations.

Table 5.3: *Experimental test results of beams with rectangular holes.*

Test series notation	Beam $H \times T$ [mm^2]	Hole design $a \times b$ [mm^2]	r [mm]	$\frac{D}{H}$ [-]	$\frac{M}{VH}$ [-]	n	V_{c0} Mean [kN]	V_c Mean [kN]	V_f Mean [kN]
BEN-2	500 × 90	300 × 150	0	0.67	1.20	2			39.0
BEN-4	500 × 90	200 × 100	0	0.45	1.20	2			49.6
FRE-1	550 × 80	250 × 250	?	0.64	0.91	2			32.7
FRE-2	550 × 80	250 × 150	?	0.53	0.91	2			44.0
FRE-3	550 × 80	250 × 250	?	0.64	1.82	2			33.8
FRE-4	550 × 80	250 × 150	?	0.53	1.82	2			35.4
PENa-4	500 × 90	200 × 200	?	0.57	1.60	1			33.8
PENa-5	500 × 90	400 × 200	?	0.89	1.60	1	25.0		31.3
PENa-6	500 × 90	600 × 200	?	1.26	1.60	1	20.8		30.0
PENb-3	800 × 115	400 × 200	?	0.56	1.25	1			69.1
PENb-4	800 × 115	200 × 200	?	0.35	1.25	1	52.5		84.4
JOHa-2	500 × 90	250 × 250	25	0.71	1.30	2		26.8	28.5
JOHa-4	500 × 90	250 × 250	25	0.71	2.80	2		22.2	25.6
JOHc-1	400 × 140	600 × 200	25	1.58	2.25	1		30.0	37.0
JOHd-3	495 × 88	125 × 125	25	0.36	2.53	4		40.4	
JOHd-4	495 × 88	375 × 125	25	0.80	2.53	4		37.7	
JOHd-5	495 × 88	370 × 370	25	1.06	2.53	4		9.1	
JOHd-6	495 × 88	735 × 245	25	1.57	2.53	4		12.5	
JOHd-7	495 × 88	1110 × 370	25	2.36	2.53	4		4.2	
PIZa-1	400 × 120	180 × 180	0	0.64	1.05	2	24.1	30.6	63.7
PIZa-2	400 × 120	180 × 90	0	0.50	1.05	2	37.2	54.9	75.5
PIZa-3	400 × 120	180 × 10	0	0.45	1.05	2	95.2	103.3	103.3
PIZb-1	400 × 120	180 × 90	0	0.50	1.05	1	56.6	71.0	84.5
PIZc-1	400 × 120	180 × 10	0	0.45	1.05	1	110.1	110.1	110.1
PIZd-1	400 × 120	360 × 180	0	1.01	1.75	2	21.7	23.3	24.8
PIZd-2	400 × 120	10 × 180	0	0.45	1.75	1	34.0	34.0	34.0
PIZe-1	400 × 120	360 × 180	0	1.01	1.75	1	19.2	21.1	28.8
PIZe-2	400 × 120	10 × 180	0	0.45	1.75	2	30.0	33.8	33.8
PIZe-3	400 × 120	180 × 90	0	0.50	1.75	3	45.8	54.2	54.2
PIZf-1	400 × 120	180 × 180	0	0.64	1.05	2	20.6	26.8	70.0
HALa-1	315 × 90	400 × 150	25	1.36	2.78	5		11.9	
HALa-2	315 × 90	400 × 150	0	1.36	2.78	5		12.2	
HALb-1	315 × 90	400 × 150	25	1.36	2.78	5		12.2	
HALc-1	315 × 90	400 × 150	25	1.36	?	1		12.2	
HALd-1	585 × 165	600 × 295	25	1.14	?	4		27.1	

Test series notation	Limträhandbok Method 1 V_k [kN]	V_c/V_k [-]	Limträhandbok Method 2 V_k [kN]	V_c/V_k [-]	DIN 1052 2004 V_k [kN]	V_c/V_k [-]	DIN 1052 1999 V_k [kN]	V_c/V_k [-]	SIA 265 V_k [kN]	V_c/V_k [-]
BEN-2	22.3 [3]		37.4 [3]		29.0 [3]		29.0 [3]		54.4	
BEN-4	30.8 [3]		60.7 [3]		38.4 [3]		38.4 [3]		81.5	
FRE-1	19.5		26.4		22.8 [1]		22.8 [1]		28.4	
FRE-2	28.6		42.9		31.2		31.2		56.4	
FRE-3	19.5		26.4		21.2 [1]		21.2 [1]		28.4	
FRE-4	28.6		42.9		28.6		28.6		56.4	
PENa-4	20.8		34.6		23.8		23.8		37.4	
PENa-5	16.1		24.2		23.3		23.3		37.4	
PENa-6	12.4		18.6		23.0 [1]		23.0 [1]		37.4	
PENb-3	51.0		76.3		66.7		66.7		106.9	
PENb-4	61.2		98.3		67.5		67.5		106.9	
JOHa-2	15.5	1.73	24.0	1.12	21.5 [1]	1.25	21.5 [1]	1.25	25.5	1.05
JOHa-4	15.5	1.43	24.0	0.93	19.1 [1]	1.16	19.1 [1]	1.16	25.5	0.87
JOHc-1	9.7	3.09	16.4	1.83	23.9 [1]	1.26	23.9 [1]	1.26	35.4	0.85
JOHd-3	31.4	1.29	60.8	0.66	29.3	1.38	29.3	1.38	66.1	0.61
JOHd-4	21.7	1.73	38.5	0.98	28.7	1.31	28.7	1.31	66.1	0.57
JOHd-5	6.2 [1]	1.47	8.1 [1]	1.12	15.5 [1]	0.59	15.5 [1]	0.59	7.8	1.17
JOHd-6	8.8	1.42	12.4	1.01	19.1 [1]	0.65	19.1 [1]	0.65	26.5	0.47
JOHd-7	2.9 [1]	1.45	3.3 [1]	1.27	14.5 [1]	0.29	14.5 [1]	0.29	7.8	0.54
PIZa-1	18.1 [3]	1.69	34.4 [3]	0.89	24.7 [1,3]	1.24	24.7 [1,3]	1.24	36.9	0.83
PIZa-2	28.6 [3]	1.92	63.6 [3]	0.86	38.2 [3]	1.44	38.2 [3]	1.44	87.3	0.63
PIZa-3	37.7 [1,3]	2.74	124.8 [1,3]	0.83	155.0 [3]	0.67	155.0 [3]	0.67	124.8	0.83
PIZb-1	28.6 [3]	2.48	63.6 [3]	1.12	38.2 [3]	1.86	38.2 [3]	1.86	87.3	0.81
PIZc-1	37.7 [1,3]	2.92	124.8 [1,3]	0.88	155.0 [3]	0.71	155.0 [3]	0.71	124.8	0.88
PIZd-1	13.7 [3]	1.70	23.4 [3]	1.00	23.0 [1,2,3]	1.01	23.0 [1,2,3]	1.01	36.9	0.63
PIZd-2	21.3 [3]	1.60	62.0 [3]	0.55	23.8 [1,3]	1.43	23.8 [1,3]	1.43	36.9	0.92
PIZe-1	13.7 [3]	1.54	23.4 [3]	0.90	23.0 [1,2,3]	0.92	23.0 [1,2,3]	0.92	36.9	0.57
PIZe-2	21.3 [3]	1.59	62.0 [3]	0.55	23.7 [1,3]	1.43	23.7 [1,3]	1.43	36.9	0.92
PIZe-3	28.6 [3]	1.90	63.6 [3]	0.53	35.6 [3]	0.95	35.6 [3]	0.95	87.3	0.39
PIZf-1	18.1 [3]	1.48	34.4 [3]	0.78	24.7 [1,3]	1.09	24.7 [1,3]	1.09	36.9	0.73
HALa-1	6.4	1.86	11.4	1.04	12.0 [1]	0.99	12.0 [1]	0.99	22.2	0.54
HALa-2	6.4 [3]	1.91	11.4 [3]	1.07	12.0 [1,3]	1.02	12.0 [1,3]	1.02	22.2	0.55
HALb-1	6.4	1.91	11.4	1.07	12.0 [1]	1.02	12.0 [1]	1.02	22.2	0.55
HALc-1	6.4	1.91	11.4	1.07	- [1,4]		- [1,4]		22.2	0.55
HALd-1	21.1 [1]	1.28	30.5 [1]	0.89	- [1,4]		- [1,4]		49.6	0.55

[1] = Size of hole not within regulations.
[2] = Placement of hole not within regulations.
[3] = Radius of corner not within regulations.
[4] = Vital test data missing.

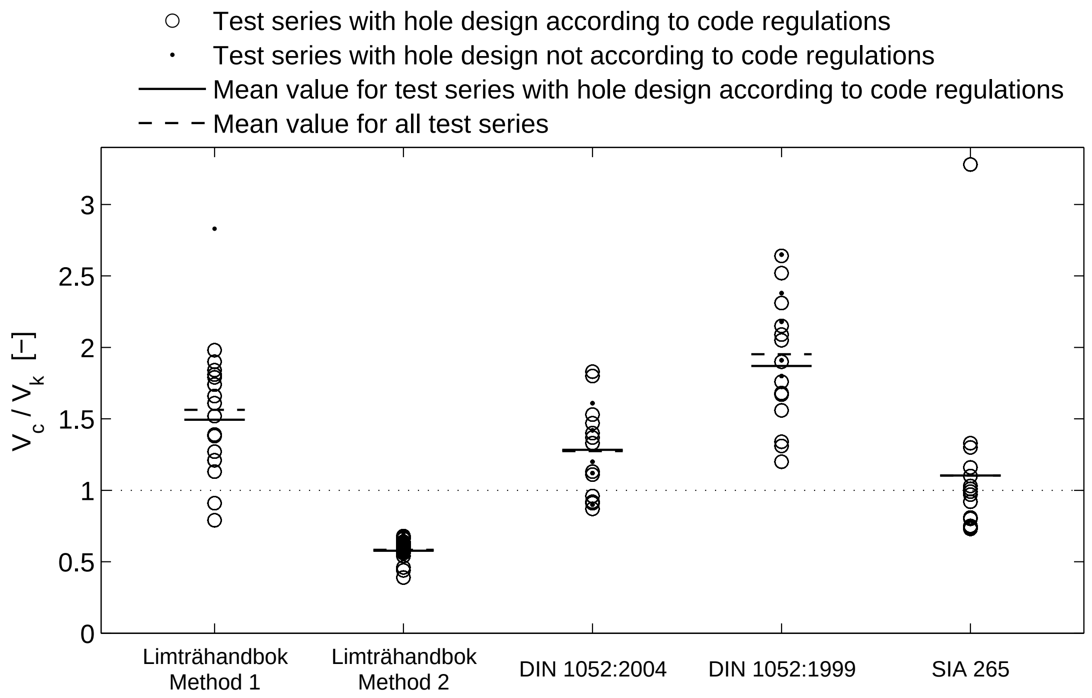

Figure 5.6: *Ratio between mean crack load V_c from experimental tests on test series with circular holes and characteristic capacity V_k according to codes.*

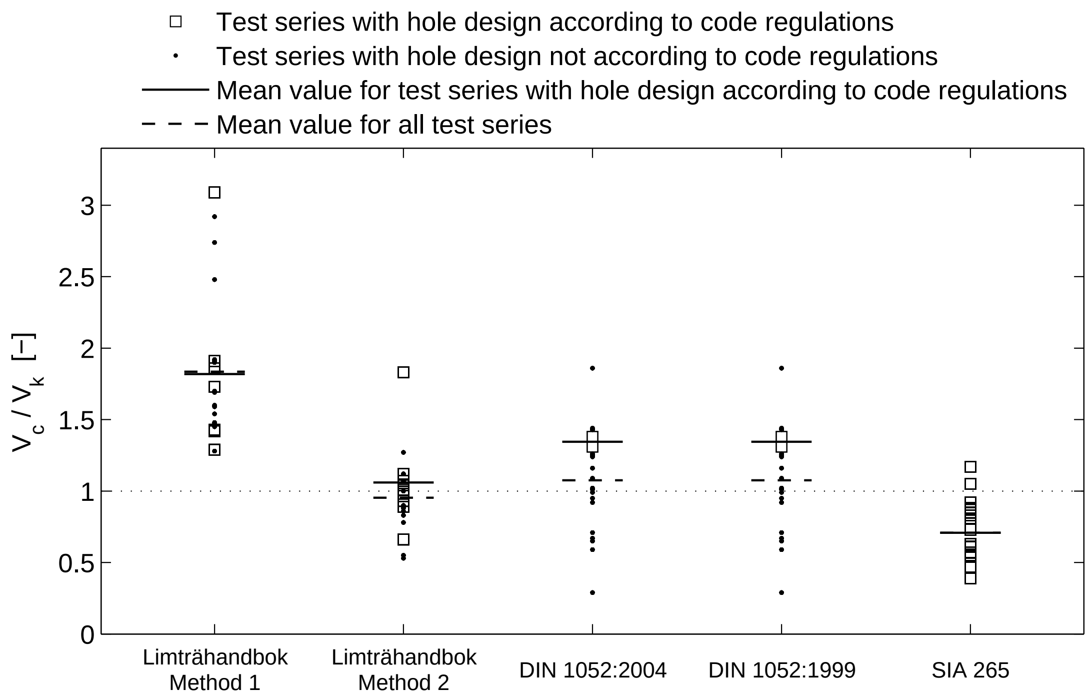

Figure 5.7: *Ratio between mean crack load V_c from experimental tests on test series with rectangular holes and characteristic capacity V_k according to codes.*

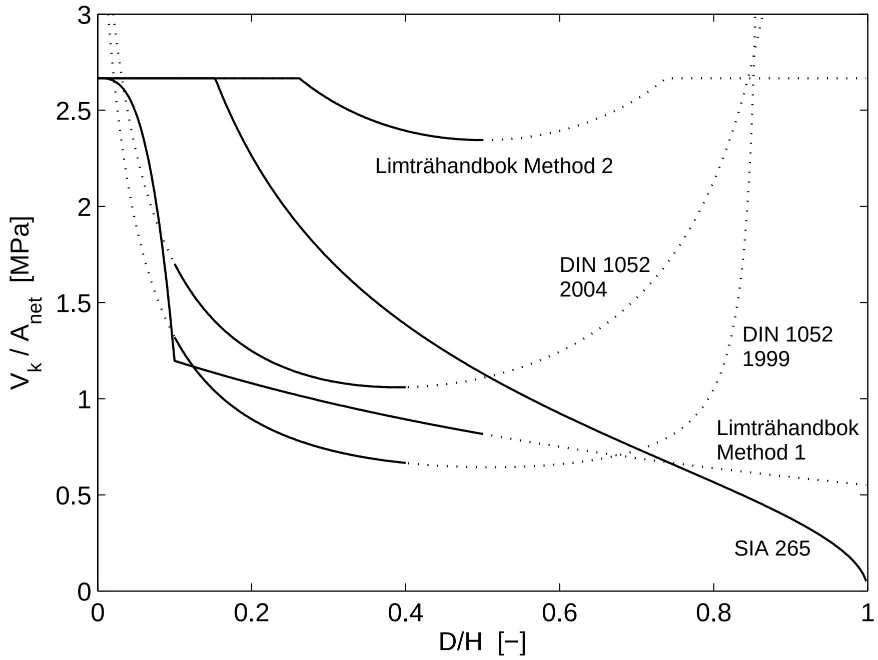

Figure 5.8: *Characteristic capacity V_k/A_{net} according to codes for beams with cross section $H \times T = 500 \times 90$ mm^2 and with circular holes ($D = \phi$). The curves for DIN 1052 are based on $M/(VH) = 2.0$.*

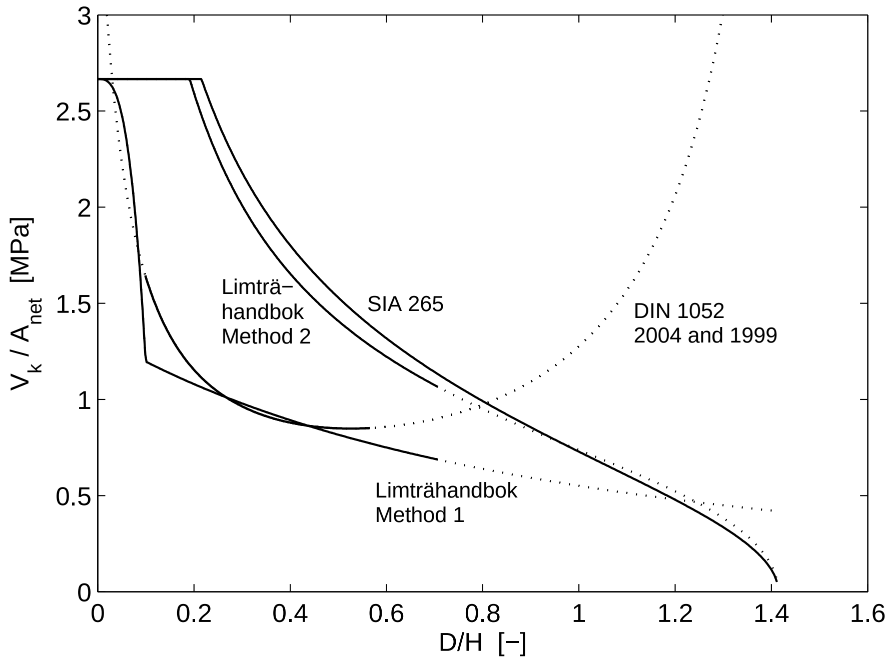

Figure 5.9: *Characteristic capacity V_k/A_{net} according to codes for beams with cross section $H \times T = 500 \times 90$ mm^2 and with quadratic holes ($D = \sqrt{a^2 + b^2}$, $a = b$). The curves for DIN 1052 are based on $M/(VH) = 2.0$.*

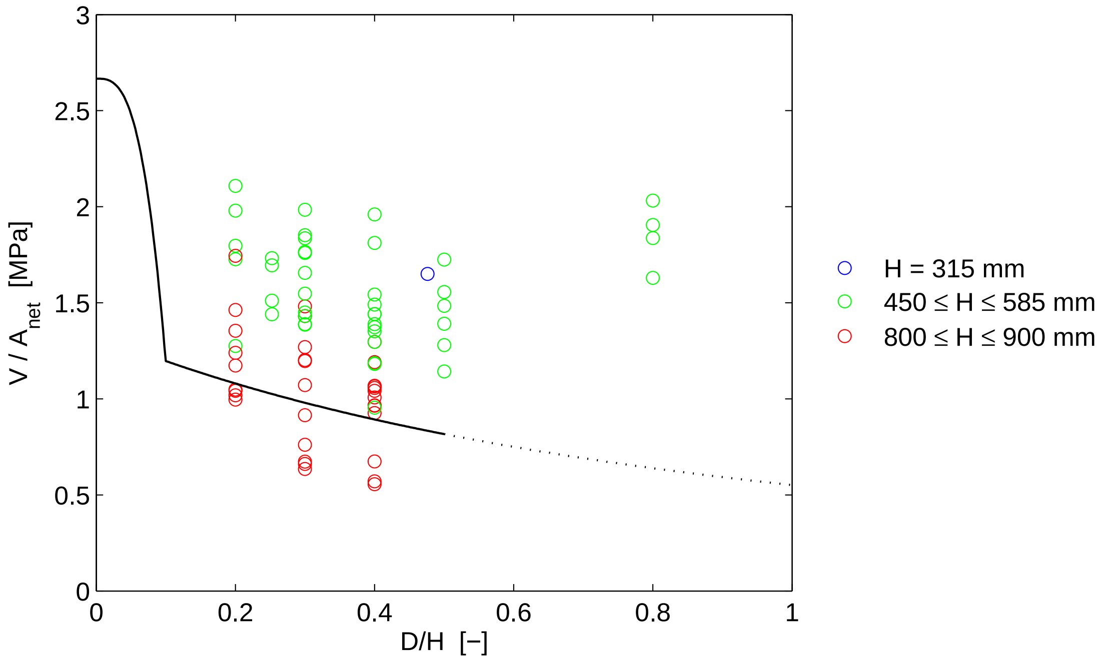

Figure 5.10: *Characteristic capacity V_k/A_{net} according to Limträhandbok method 1 compared to V_c/A_{net} for experimental tests on circular holes ($D = \phi$). V_k/A_{net} valid for all beam heights H and based on beam width $T = 90$ mm.*

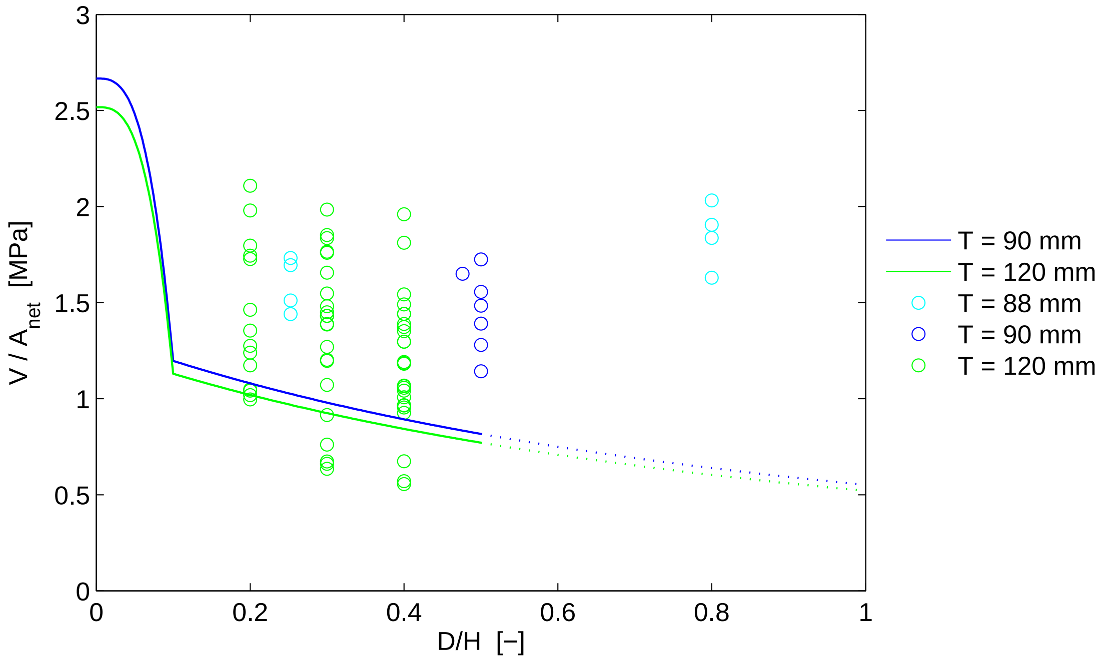

Figure 5.11: *Characteristic capacity V_k/A_{net} according to Limträhandbok method 1 for different beam widths T compared to V_c/A_{net} for experimental tests on circular holes ($D = \phi$).*

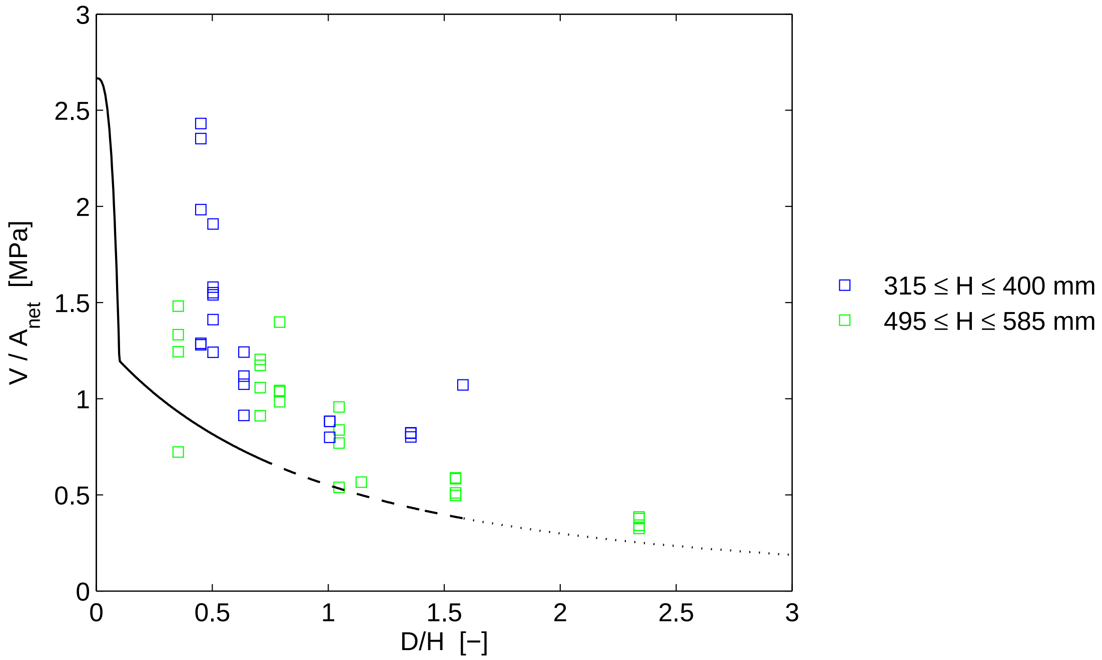

Figure 5.12: *Characteristic capacity V_k/A_{net} according to Limträhandbok method 1 compared to V_c/A_{net} for experimental tests on rectangular holes ($D = \sqrt{a^2+b^2}$). V_k/A_{net} valid for all beam heights H and based on beam width $T = 90$ mm.*

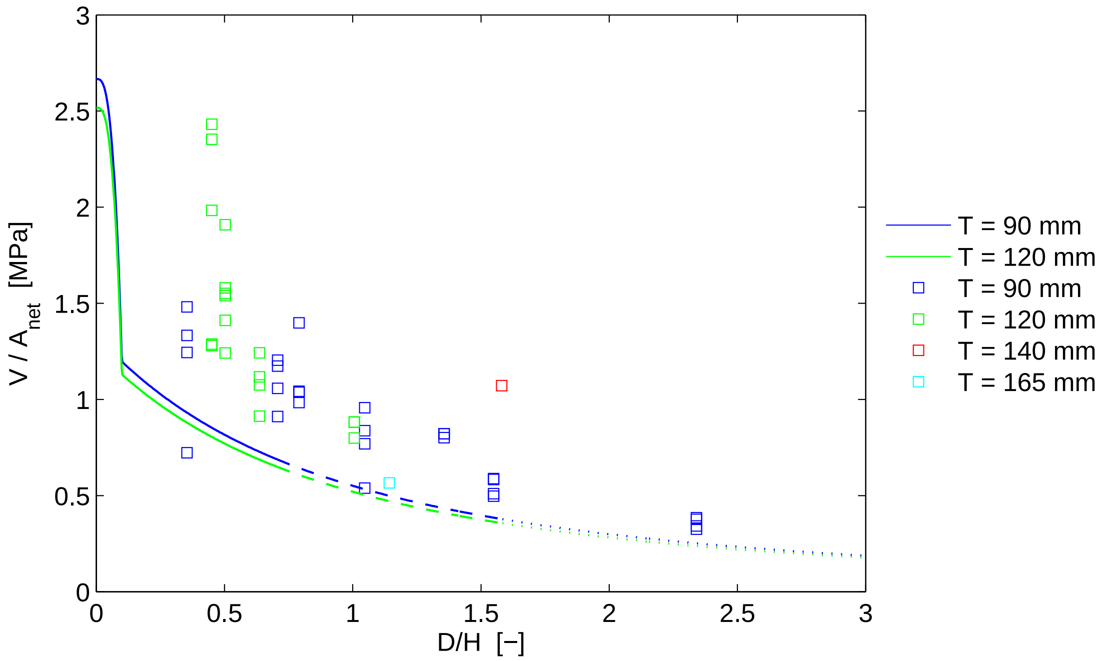

Figure 5.13: *Characteristic capacity V_k/A_{net} according to Limträhandbok method 1 for different beam widths T compared to V_c/A_{net} for experimental tests on rectangular holes ($D = \sqrt{a^2+b^2}$).*

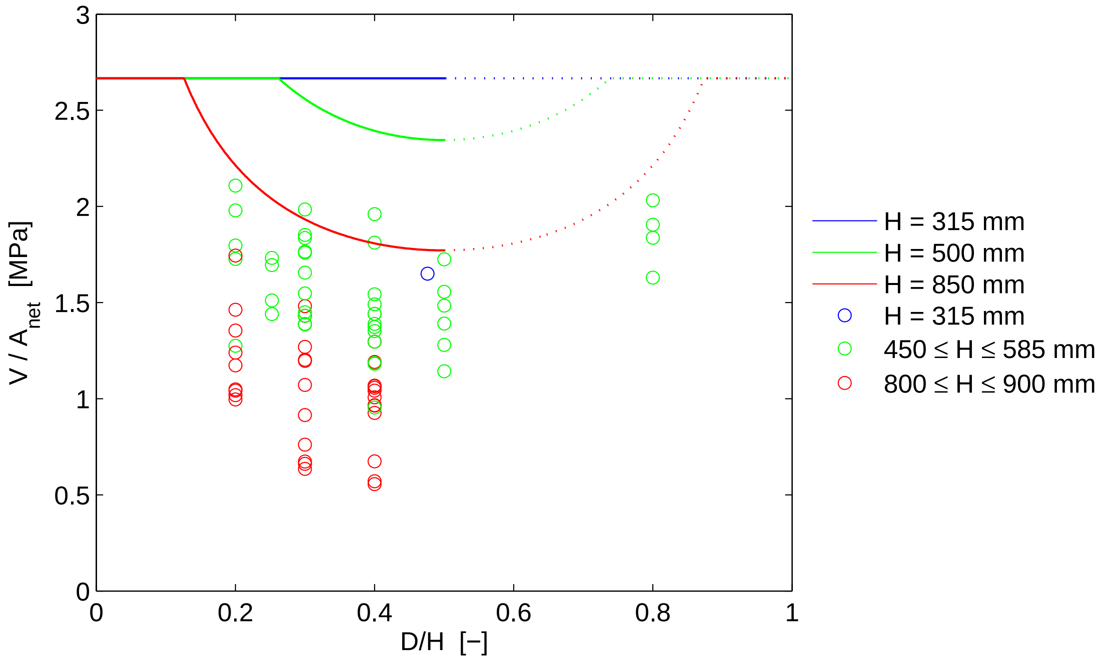

Figure 5.14: *Characteristic capacity V_k/A_{net} according to Limträhandbok method 2 for different beam heights compared to V_c/A_{net} for experimental tests on circular holes ($D = \phi$).*

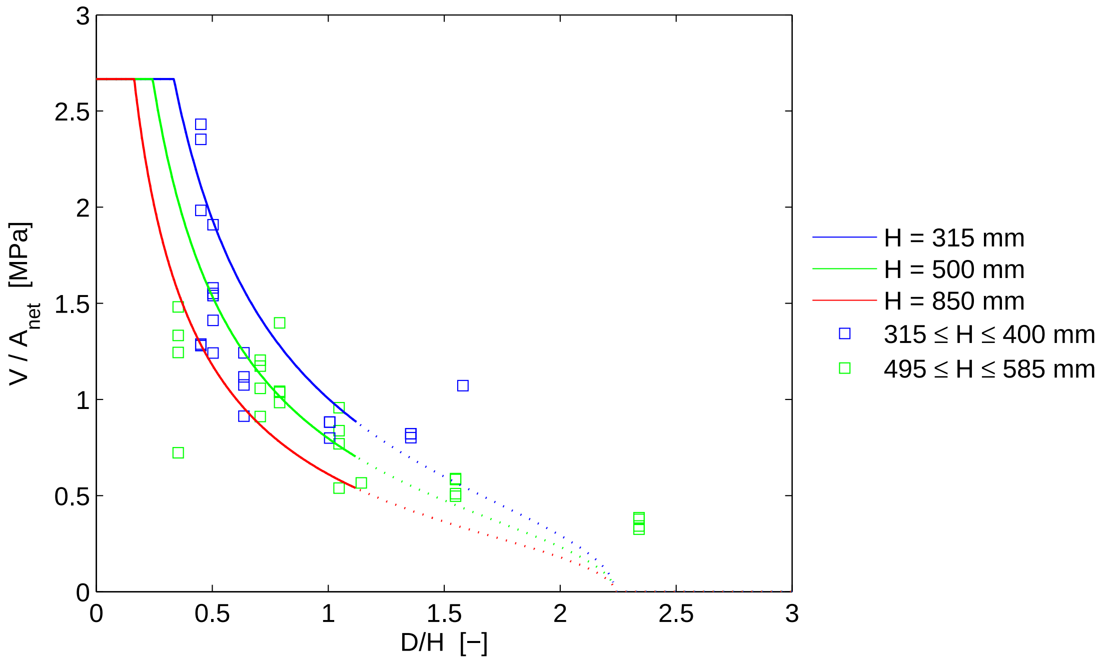

Figure 5.15: *Characteristic capacity V_k/A_{net} according to Limträhandbok method 2 for different beam heights compared to V_c/A_{net} for experimental tests on rectangular holes ($D = \sqrt{a^2 + b^2}$). V_k/A_{net} based on hole side length ratio $a/b = 2.0$.*

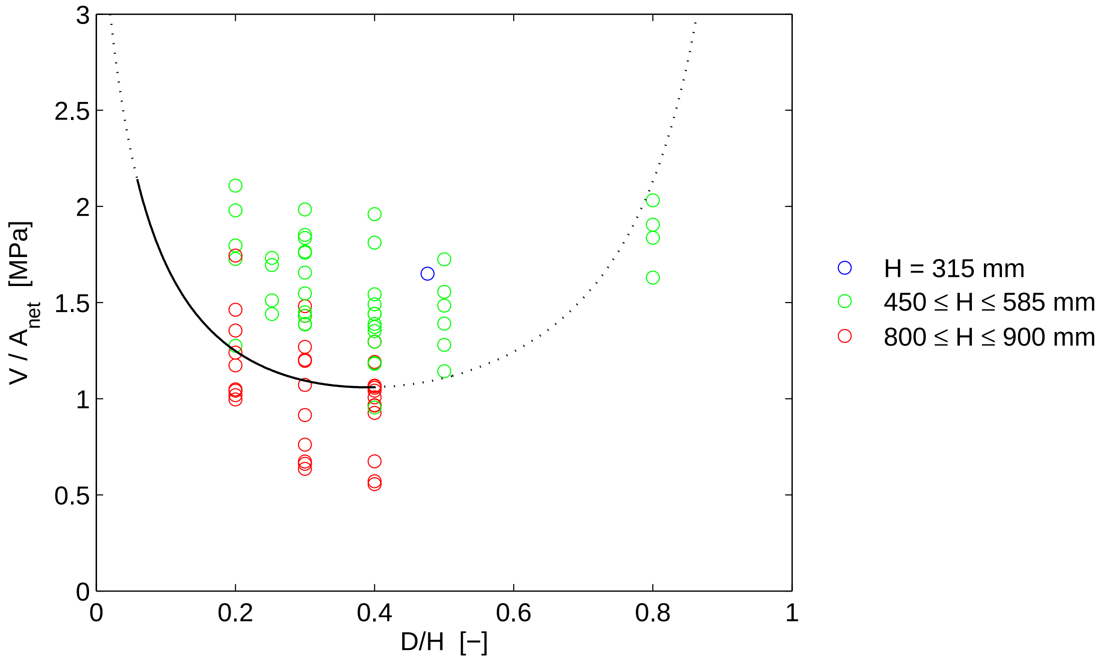

Figure 5.16: *Characteristic capacity V_k/A_{net} according to DIN 1052:2004 compared to V_c/A_{net} for experimental tests on circular holes ($D = \phi$). V_k/A_{net} valid for all beam heights H and based on bending moment to shear force ratio $M/(VH) = 2.0$.*

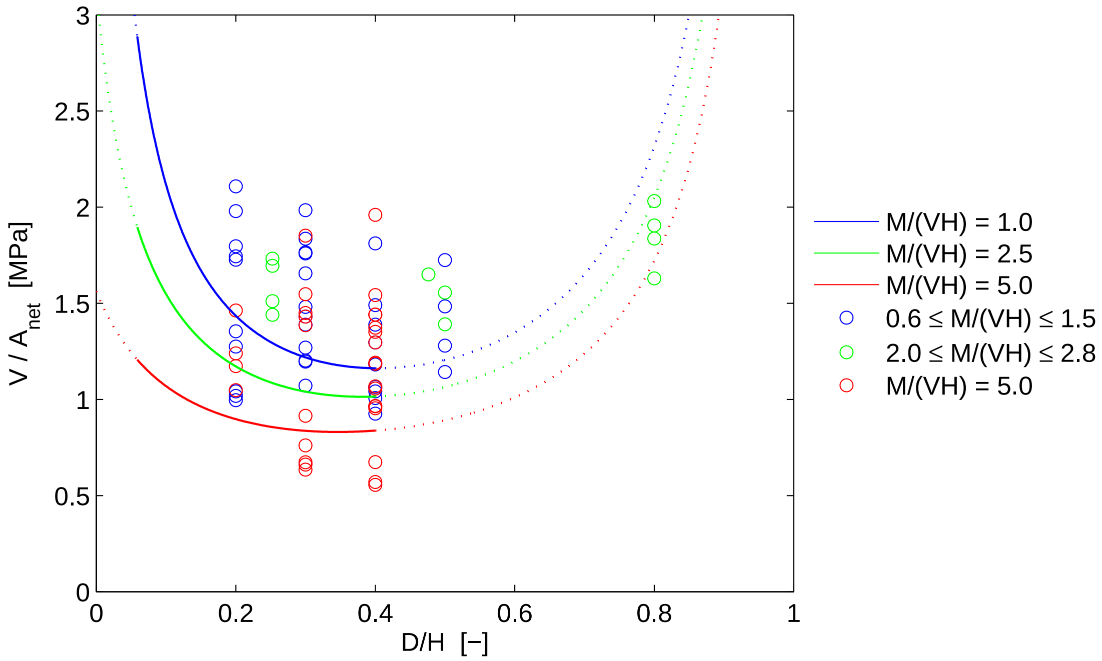

Figure 5.17: *Characteristic capacity V_k/A_{net} according to DIN 1052:2004 for different bending moment to shear force ratio $M/(VH)$ compared to V_c/A_{net} for experimental tests on circular holes ($D = \phi$). V_k/A_{net} valid for all beam heights H.*

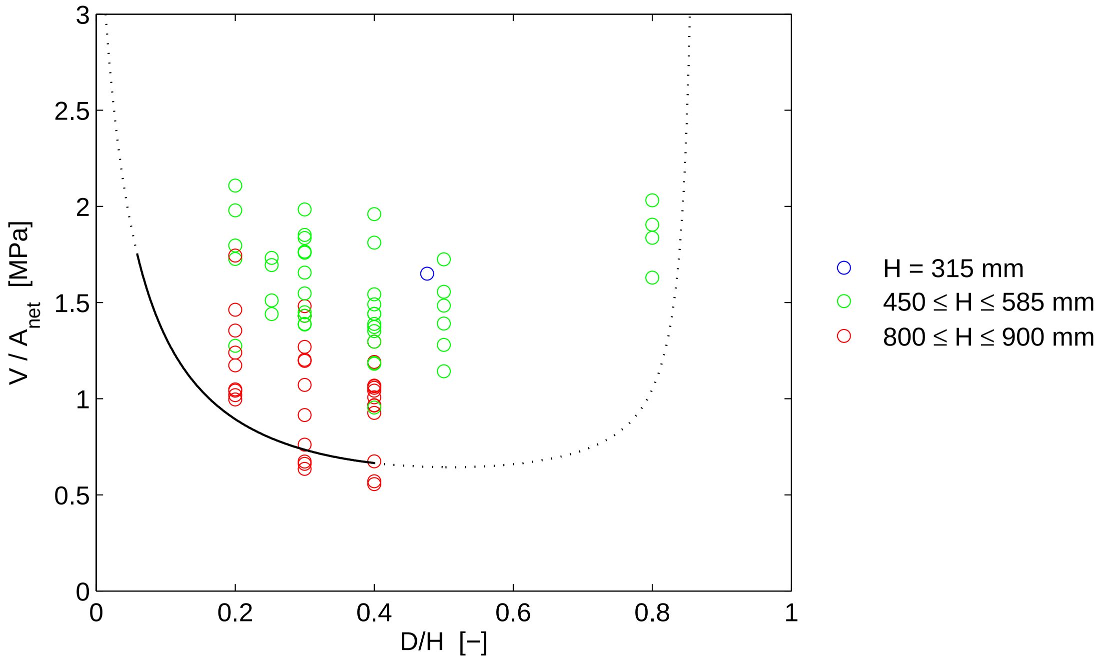

Figure 5.18: *Characteristic capacity V_k/A_{net} according to DIN 1052:1999 compared to V_c/A_{net} for experimental tests on circular holes ($D = \phi$). V_k/A_{net} valid for all beam heights H and based on bending moment to shear force ratio $M/(VH) = 2.0$.*

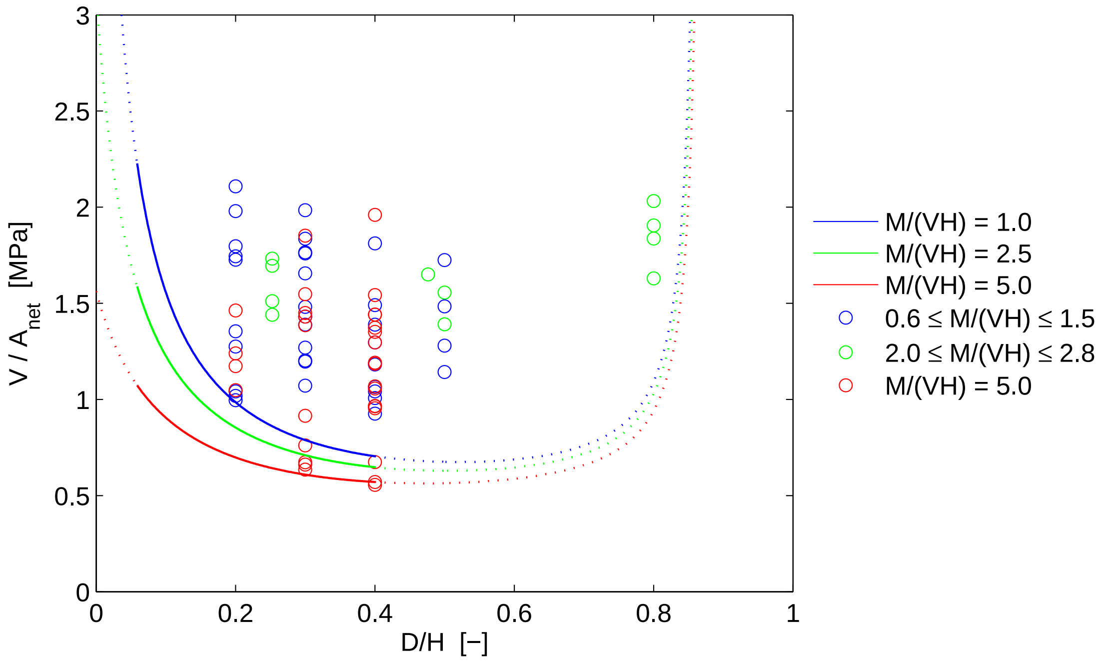

Figure 5.19: *Characteristic capacity V_k/A_{net} according to DIN 1052:1999 for different bending moment to shear force ratio $M/(VH)$ compared to V_c/A_{net} for experimental tests on circular holes ($D = \phi$). V_k/A_{net} valid for all beam heights H.*

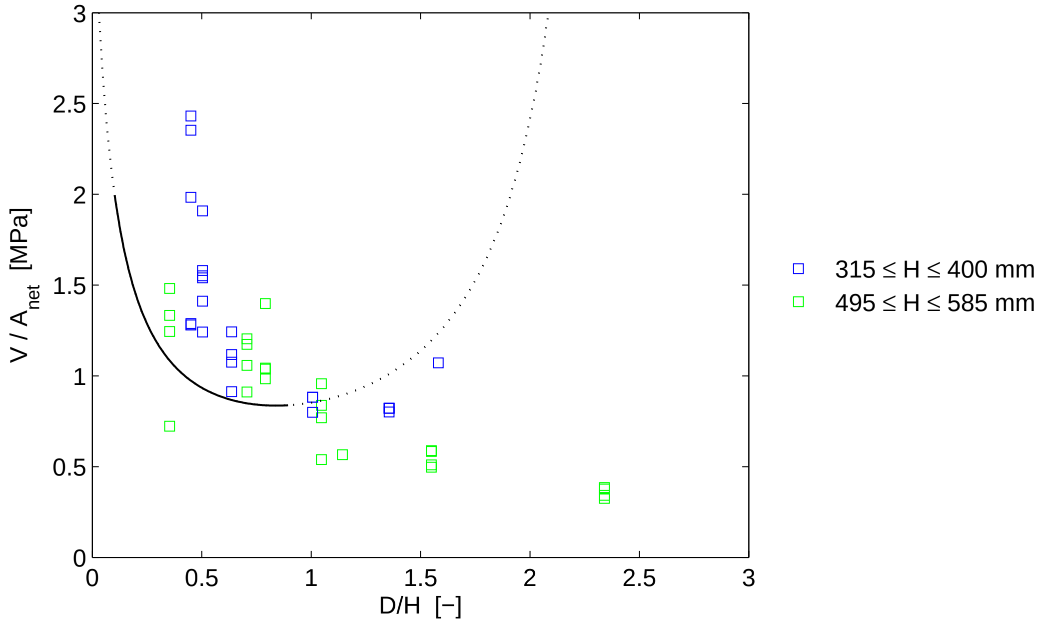

Figure 5.20: *Characteristic capacity* V_k/A_{net} *according to DIN 1052:2004 and DIN 1052:1999 compared to* V_c/A_{net} *for experimental tests on rectangular holes* ($D = \sqrt{a^2+b^2}$)*.* V_k/A_{net} *valid for all beam heights* H *and based on bending moment to shear force ratio* $M/(VH) = 2.0$ *and on hole side length ratio* $a/b = 2.0$.

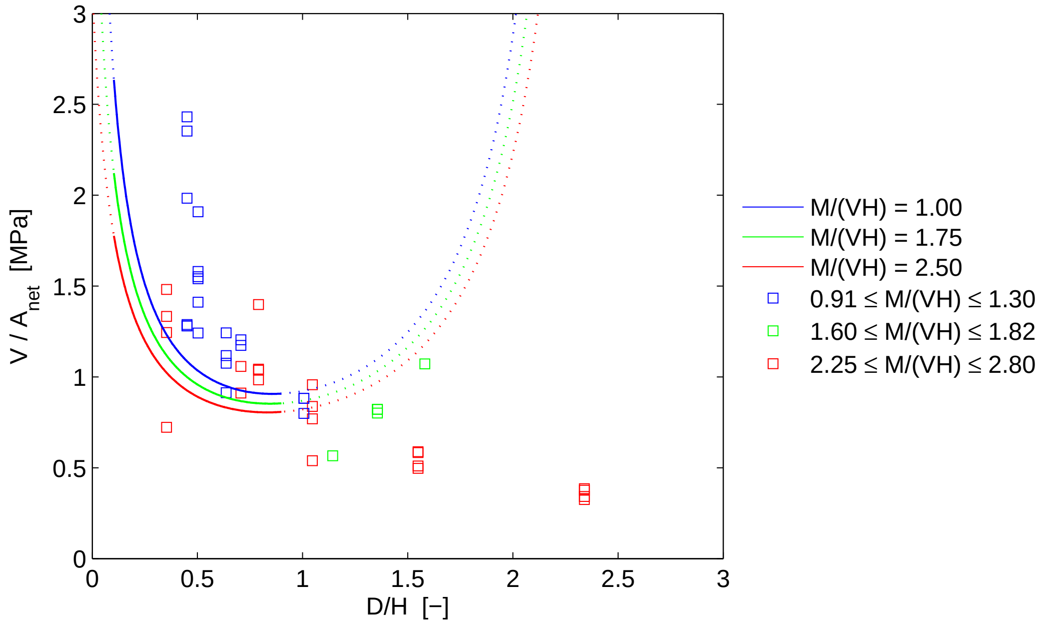

Figure 5.21: *Characteristic capacity* V_k/A_{net} *according to DIN 1052:2004 and DIN 1052:1999 for different bending moment to shear force ratio* $M/(VH)$ *compared to* V_c/A_{net} *for experimental tests on rectangular holes* ($D = \sqrt{a^2+b^2}$)*.* V_k/A_{net} *valid for all beam heights* H *and based on hole side length ratio* $a/b = 2.0$.

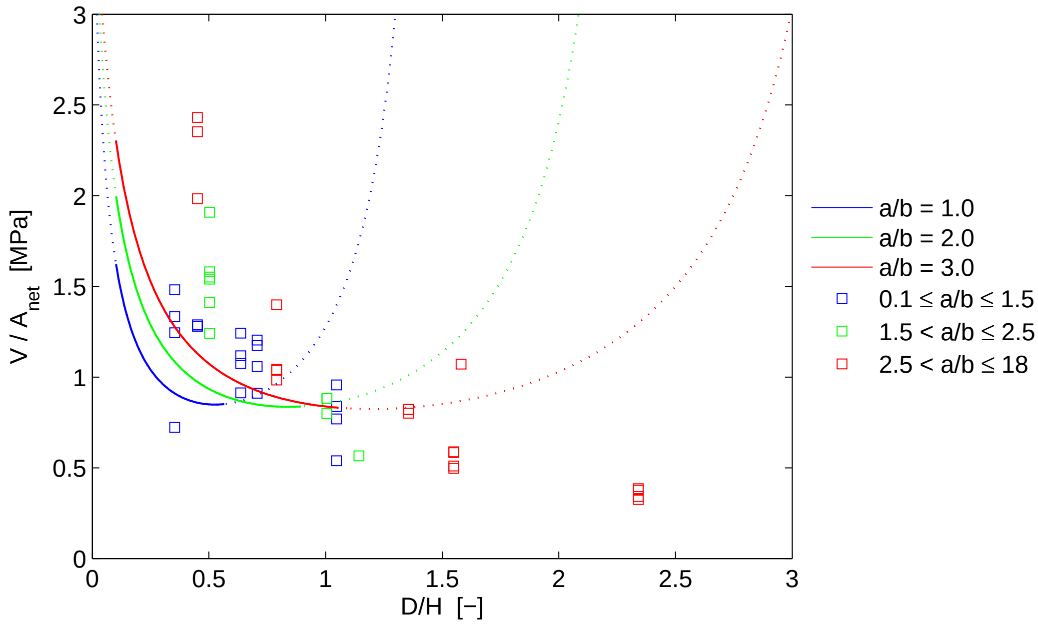

Figure 5.22: *Characteristic capacity V_k/A_{net} according to DIN 1052:2004 and DIN 1052:1999 for different hole side ratios a/b compared to V_c/A_{net} for experimental tests on rectangular holes ($D = \sqrt{a^2 + b^2}$). V_k/A_{net} valid for all beam heights H and based on bending moment to shear force ratio $M/(VH) = 2.0$.*

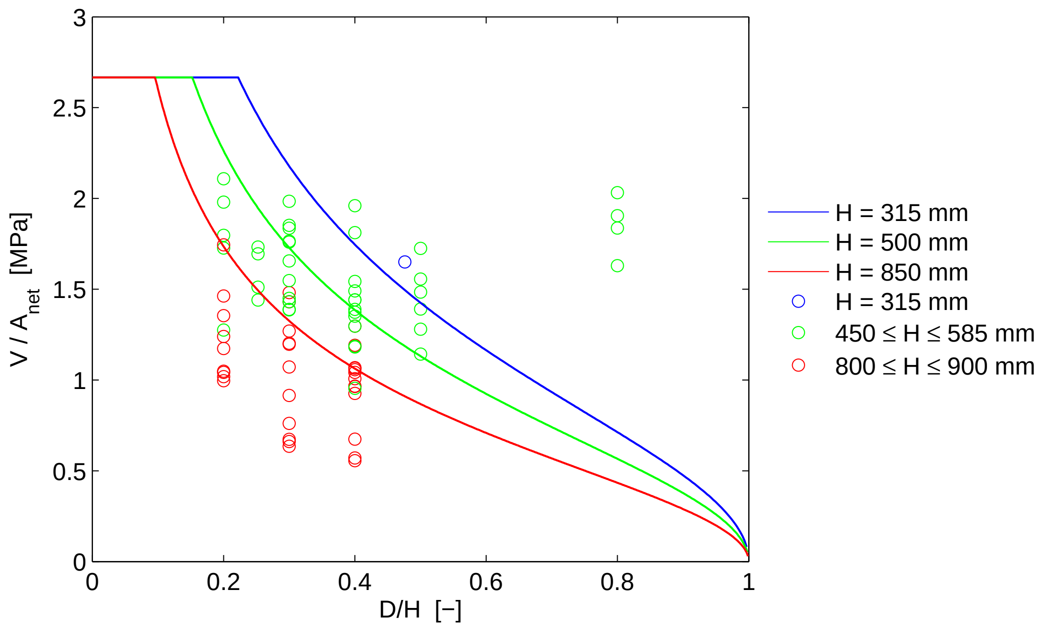

Figure 5.23: *Characteristic capacity V_k/A_{net} according to SIA 265 for different beam heights compared to V_c/A_{net} for experimental tests on circular holes ($D = \phi$).*

Chapter 6

Concluding remarks

Several experimental and theoretical investigations have been carried out on the load bearing capacity of glulam beams with a hole. This can be explained by the need for reliable strength design methods and perhaps also by beams with a hole serving as a vehicle in relation to more general research on strength analysis of wooden structural elements.

Concluding remarks concerning experimental tests

A vast majority of the tests results presented in literature concern straight beams with constant height (176 out of 182). The cross section of all beams vary within the ranges of $80 \leq T \leq 165$ mm and $315 \leq H \leq 900$ mm. All tested beams had holes which were centrically placed with respect to the height of the beam and most holes were placed in parts of the beams that are dominated by shear force but there are also tests on holes subjected to pure bending. Minor differences between test setups, test procedures and material are of course a weak point in the comparison of different test series. There are also some investigations of beams with reinforcement but these are however in general not included in this compilation since it focuses on unreinforced holes.

From the mean values of the crack initiation load, the crack load and the failure load presented in Tables 2.27 and 2.28 it may seem like failures in general are not very sudden since the for most cases $V_{c0} < V_c < V_f$. However, looking at the individual tests it can be seen that for a number of beams the difference between the crack initiation load and the failure load is small and for some beams there is no difference.

Concluding remarks concerning calculations approaches

Most of the theoretical strength analysis methods applied to beams with a hole are simplified by using a linear elastic two dimensional model assuming a plane state of stress. The calculated perpendicular to grain stresses are then to be considered as a mean stress over the beam width. Höfflin's [12] three dimensional finite element calculations however shows that the perpendicular to grain stresses vary significantly across the beam width. Fracture criteria based on stress and on linear elastic fracture mechanics parameters have been applied.

Concluding remarks concerning design codes

The design rules presented in Chapter 5 show fundamental dissimilarities concerning the design approaches. The analogy between a hole and an end-notched beam is used in some of the codes presented although the state of stresses differs in many ways. Other presented procedures are instead empirically based. As can be seen in Tables 5.2 and 5.3, also the computed characteristic strengths V_k for beams with holes in shear force dominated region varies significantly between the different codes and the ratio V_c/V_k also varies within rather wide ranges for most of the codes. One exception is design of circular holes according method 2 in *Limträhandbok*. This method, based on design of end-notched beams, in general predicts the highest shear force capacity of the presented codes but the variation of V_c/V_k between the test series is comparatively small. Method 1 according to *Limträhandbok*, which is empirically based, seems to predict values on the safe side ($V_c < V_k$) for all but two test series. These exceptions are test series with large beams ($H = 900$ mm) with comparatively high bending moment to shear force ratio ($M/(VH) = 5$). There is no beam height size effect taken into account in method 1 from *Limträhandbok* or in DIN 1052. The contemporary version of the German code overestimates the capacity for five test series with circular holes, four of these are test series with large beams ($H = 900$ mm) while the fifth test series has a hole twice the allowed size. In a majority of the test series with rectangular holes, the hole size or corner radius are not within regulations stated in the code.

Concluding remarks concerning lack of knowledge

Although the investigations all in all represent much work, it seems that this work essentially has been concentrated on a narrow field restricted by quantities related to:

- *Beam geometry*
  The investigations consists predominantly of straight beams with constant height and with centrically placed holes. A few curved beams have been tested but it seem as tapered beams with holes have not been investigated. Neither has small beams ($H < 315$ mm) or large beams ($H > 900$ mm) been tested.

- *Mode of loading*
  Only in-plane shear and bending have been studied. Thus, little is known about hole induced strength reduction for a beam in tension, compression, torsion and out of plane (flatwise) shear and/or bending.

- *Moisture effects*
  It is very likely that drying significantly decreases the cracking load and most probably also the failure load of a beam with a hole. It is obvious that moisture

gradients in the vicinity of the hole can give additional stresses. A homogeneous change in moisture level can also give such parasite stresses due to the heterogenous character of wood. In spite of this, it seems that no tests have been carried out on influence of moisture change.

- *Duration of load*
  It seems like very few tests have been carried out on duration of load effects and it also seems like the possible influence of cyclic loading, i.e. fatigue, is yet to be investigated.

Further development of simulation tools and strength modeling methods are also needed in order to increase the possibilities to understand and predict the strength of beams with holes. The most comprehensive recent advanced theoretical study is probably the study of beams with circular holes by means of Weibull-modeling and finite elements presented by Höfflin [12]. Further modeling development should aim for consideration of the influence of the fracture toughness or fracture energy of the wood, the influence of moisture effects and the desire for a unified approach for modeling of both circular and rectangular holes with more or less sharp corners.

Bibliography

[1] Aicher S., Schmidt J., Brunhold S.
Design of timber beams with holes by means of fracture mechanics.
CIB-W18/28-19-4, Copenhagen, Denmark, 1995.

[2] Aicher S., Höfflin L.
Tragfähigkeit und Bemessung von Brettschichtholzträgern mit runden Durchbrüchen – Sicherheitsrelevante Modifikationen der Bemessungsverfahren nach Eurocode 5 und DIN 1052. (In German)
(Load capacity and design of glulam beams with round holes – Safety relevant modifications of design methods according to Eurocode 5 and DIN 1052.)
MPA Otto-Graf-Institute, University of Stuttgart, 2006.

[3] Aicher S., Gustafsson P.J., Haller P., Petersson H.
Fracture mechanics models for strength analysis of timber beams with a hole or a notch – A report of RILEM TC-133.
Report TVSM-7134, Division of Structural Mechanics, LTH, Lund University, 2002.

[4] Bengtsson S., Dahl G.
Inverkan av hål nära upplag på hållfastheten hos limträbalkar. (In Swedish)
(Influence of holes near support on the strength of glulam beams.)
Master's Thesis, Byggnadsteknik II, LTH, Lund University, 1971.

[5] Gustafsson P.J., Petersson H., Stefansson F.
Fracture Analysis of Wooden Beams with Holes and Notches.
Proceedings of the International Wood Engineering Conference,
Volume 4, p. 281-287, New Orleans, Louisiana, USA, 1996.

[6] Gustafsson P.J., Serrano E.
Fracture Mechanics in timber engineering – Some methods and applications.
Proceedings of 1st RILEM Symposium on Timber Engineering,
p. 141-150, Stockholm, Sweden, 1999.

[7] Gustafsson P.J., Serrano E.
Fracture Mechanics in timber engineering – Strength analysis of components and joints.
DOI 10.1617/s11527-006-9121-0, Materials and Structures, RILEM, 2006.

[8] Hallström S.
Glass fibre reinforcemed laminated timber beams with holes.
Report 95-12, Department of Lightweight Structures,
Royal Institute of Technology (KTH), Stockholm, 1995.

[9] Hallström S.
Glass fibre reinforcement around holes in laminated timber beams.
Report 95-14, Department of Lightweight Structures,
Royal Institute of Technology (KTH), Stockholm, 1995.

[10] Hellan K.
Introduction to fracture mechanics.
McGraw-Hill, 1984.

[11] Hillerborg A., Fagerlund G.
Kompendium i Byggnadsmaterial. (In Swedish)
(Compendium in Building materials.)
Division of Building Materials, LTH, Lund University, 2002.

[12] Höfflin L.
Runde Durchbrüche in Brettschichtholzträger - Experimentelle und theoretische Untersuchungen. (In German)
(Round holes in glulam beams – Experimental and theoretical analyses.)
Dissertation, MPA Otto-Graf-Institute, University of Stuttgart, 2005.

[13] Höfflin L., Aicher S.
Weibull based design approach of round holes in glulam.
CIB-W18/36-12-2, Colorado, USA, 2003.

[14] Johannesson B.
Design problems for glulam beams with holes.
Dissertation, Division of Steel and Timber structures,
Chalmers University of Technology, Göteborg, 1983.

[15] Johannesson B.
Holes in plywood beams and glued laminated timber beams.
Publication S 77:4, Division of Steel and Timber structures,
Chalmers University of Technology, Göteborg, 1977.

[16] Johannesson B.
On the Design of Glued Laminated Timber Beams with Holes.
Publication S 78:10, Division of Steel and Timber structures,
Chalmers University of Technology, Göteborg, 1978.

[17] Johannesson B.
Tests on two glued laminated timber beams.
Publication S 80:3, Division of Steel and Timber structures,
Chalmers University of Technology, Göteborg, 1978.

[18] Johannesson B.
Spänningsberäkning av anisotropa skivor. Randintegralekvationer. Randelement. (In Swedish)
(Stress calculation of anisotropic plates. Boundary integral equations. Boundary element method.)
Publication S 80:11, Division of Steel and Timber structures,
Chalmers University of Technology, Göteborg, 1980.

[19] Johannesson B.
Limträbalkar med hål. (In Swedish)
(Glulam beams with holes.)
Publication S 83:1, Division of Steel and Timber structures,
Chalmers University of Technology, Göteborg, 1983.

[20] Kolb H., Frech P.
Untersuchungen an durchbrochenen Bindern aus Brettschichtholz. (In German)
(Analyses of glulam beams with holes.)
Holz als Roh- und Werkstoff 35, p. 125-134, 1977.

[21] Penttala V.
Reiällinen liimapuupalkki. (In Finnish)
(Glulam beams with holes.)
Publication 33, Division of Structural Engineering,
Helsinki Univeristy of Technology, Otaniemi, 1980.

[22] Petersson H.
Fracture design analysis of wooden beams with holes and notches. Finite element analysis based on energy release rate approach.
CIB-W18/28-19-3, Copenhagen, Denmark, 1995.

[23] Pizio S.
Die Anwendung der Bruchmechanik zur Bemessung von Holzbauteilen, untersucht am durchbrochen und am ausgeklinkten Träger. (In German)
(The use of fracture mechanics in design of timber structures, analysed on beams with holes and notched beams.)
Publication 91:1, Dissertation, Baustatik und Stahlbau, ETH, Zürich, 1991.

[24] Riipola K.
Timber beams with holes: Fracture mechanics approach.
Journal of Structural Engineering, Volume 121, Issue 2, p. 225-239, 1995.

[25] Riipola K.
Design of glulam beams with holes.
CIB-W18/28-12-3, Copenhagen, Denmark, 1995.

[26] Scheer C., Haase K.
Durchbrüche in Brettschichtholzträger, Teil 1: Spannungstheoretische Untersuchungen. (In German)
(Holes in glulam beams, Part 1: Theoretical stress analyses.)
Holz als Roh- und Werkstoff 58, p. 153-161, 2000.

[27] Scheer C., Haase K.
Durchbrüche in Brettschichtholzträger, Teil 2: Bruchmechanische Untersuchungen. (In German)
(Holes in glulam beams, Part 2: Fracture mechanics analyses.)
Holz als Roh- und Werkstoff 58, p. 217-228, 2000.

[28] Stefansson F.
Fracture analysis of orthotropic beams – Linear elastic and nonlinear methods.
Report TVSM-3029, Licentiate Dissertation, Division of Structural Mechanics, LTH, Lund University, 2001.

[29] Thelandersson S., Larsen H.J. et al
Timber Engineering. Chapter 7 (Gustafsson P.J.)
John Wiley & Sons, England, 2003.

[30] Wu E. M.
Application of fracture mechanics to anisotropic plates
ASME Journal of Applied Mechanics, Series E, 34-4, p. 967-974, 1964.

[31] *Handbok och formalsamling i Hållfashetslära.* (In Swedish)
Department of Solid Mechanics, Royal Institute of Technology (KTH), Stockholm, 1999.

[32] Picture from MPA Stuttgart
http://www.mpa.uni-stuttgart.de/organisation/fb_1/abt_12/abt_12_en.html
2006-12-06

Codes and Handbooks

[33] Blaß H.J., Ehlbeck J., Kreuzinger H., Steck G.
Erläuterungen zu DIN 1052:2004-08 – Entwurf, Berechnung und Bemessung von Holzbauwerken. (In German)
2nd Edition including original text. DGfH innovations- und Service GmbH, München, 2005.

[34] *DIN 1052:1999 – Entwurf, Berechnung und Bemessung von Holzbauwerken.*
(In German)
1999.

[35] Boverket
Regelsamling för konstruktion – Boverkets konstruktionsregler BKR.
(In Swedish)
Elanders Gotab, Vällingby, 2003.

[36] *SIA 265 – Holzbau.* (In German)
Schweizerischer Ingenieur- und Architektenverein, 2003.

[37] *SIA 164 – Holzbau.* (In German)
Schweizerischer Ingenieur- und Architektenverein, 1992.

[38] *Eurocode 5: Design of timber structures – Part 1-1:*
General - Common rules and rules for buildings.
EN 1995-1-1:2004 (E).

[39] *Eurocode 5: Design of timber structures – Part 1-1:*
General Rules - General rules and rules for buildings.
prEN 1995-1-1: Final Draft 2002-10-09.

[40] *Glued laminated timber – Strength classes and determination of characteristic values.* Swedish version, SS-EN 1194:1999.

[41] Carling O.
Limträhandbok. (In Swedish)
(Glulam Handbook.)
Olle Carling Ingenjörsbyrå AB, Svenskt Limträ AB, www.svensktlimtra.se, 2006-04-20.